

Modern Astronomy

Part 1. Interstellar Medium (ISM)

Lecture 3

2025 March 17 (Monday), 2PM

updated 03/15, 22:01

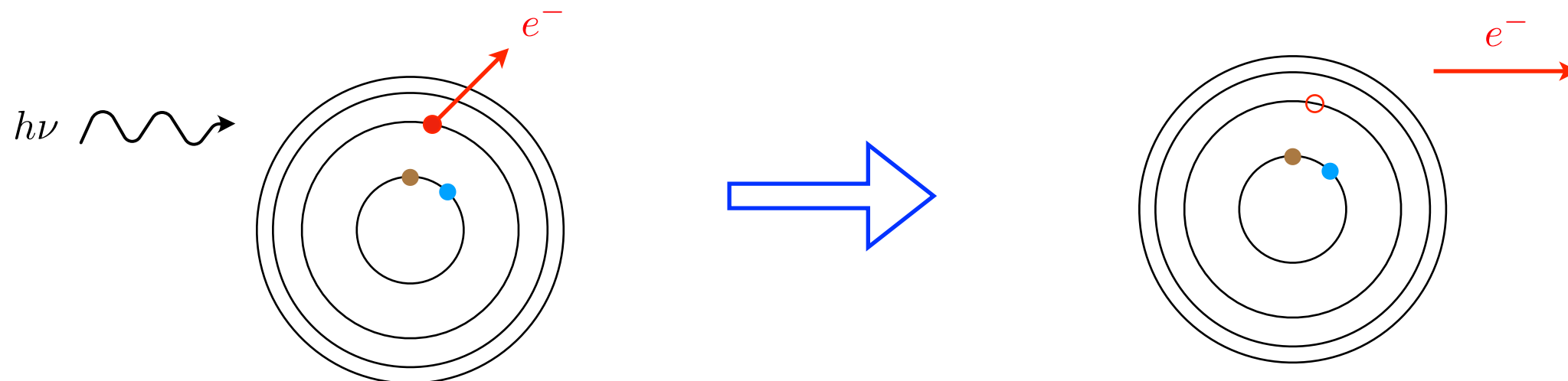
선광일 (Kwang-Il Seon)

UST / KASI

< Ionized Gas > Ionization Equilibrium

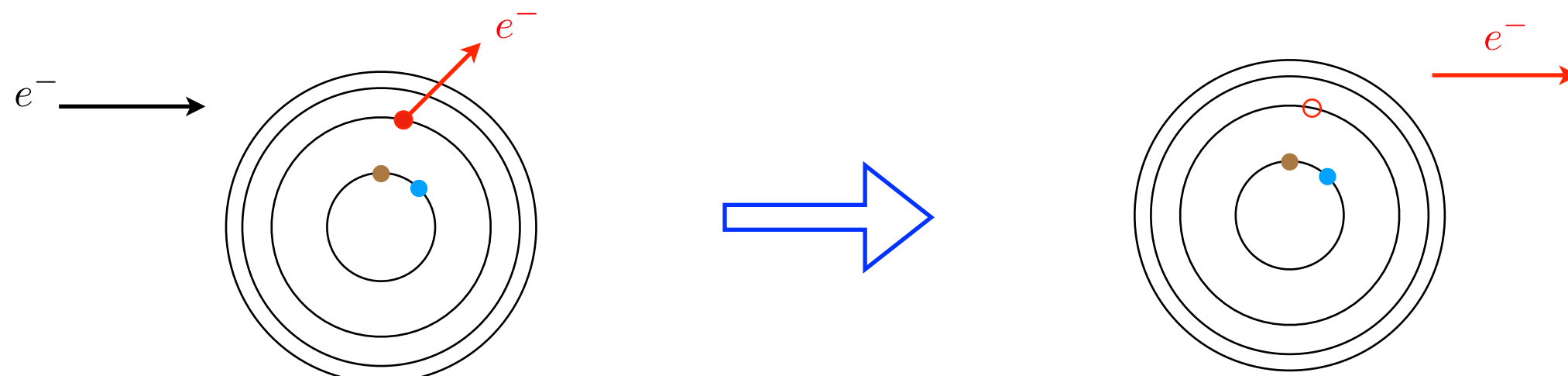
- **Photoionization Equilibrium:**

- Balance between photo-ionization and the process of recombination.



- **Collisional Ionization Equilibrium (CIE) or coronal equilibrium**

- Balance between collisional ionization from the ground states of the various atoms and ions, and the process of recombination from the higher ionization stages.
- In this equilibrium, effectively, all ions are in their ground state.

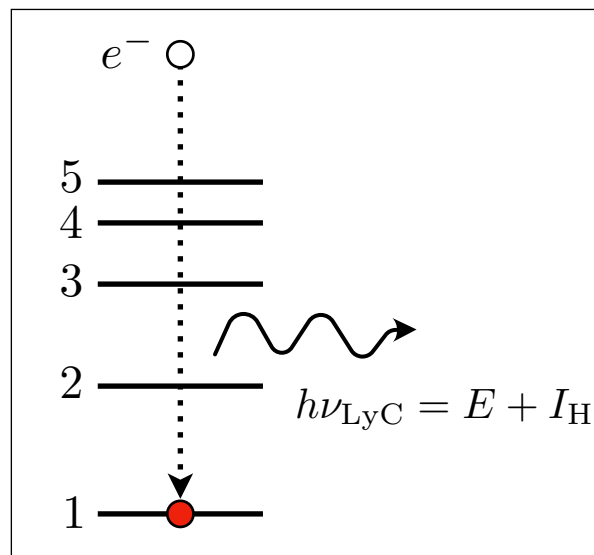


Case A and B (Radiative Recombination of Hydrogen)

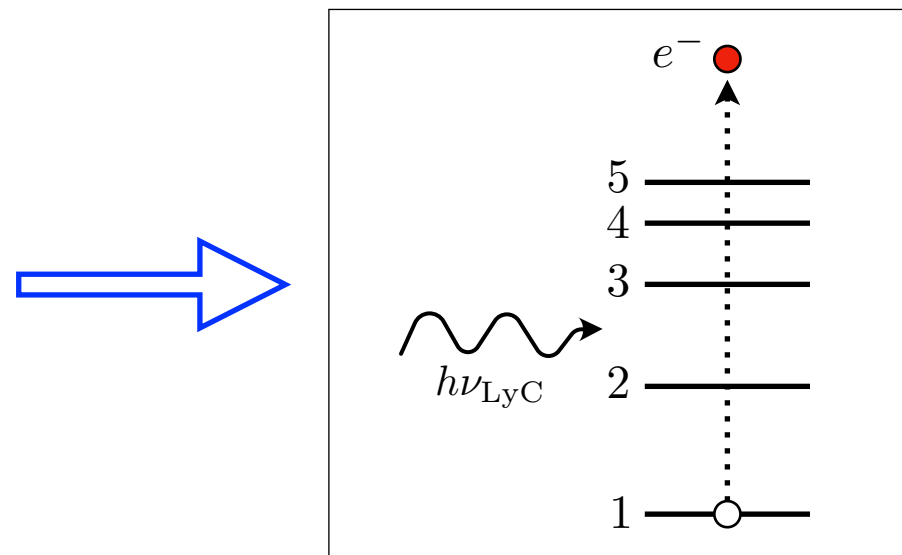
- **On-the-spot approximation:**
 - In optically thick regions, it is assumed that every photon produced by **radiative recombination to the ground state** of hydrogen is immediately, then and there, destroyed in photoionizing other hydrogen atom.
 - In the on-the-spot approximation, recombination to the ground state has no net effect on the ionization state of the hydrogen gas.
- Baker & Menzel (1938) proposed two limiting cases:
 - **Case A: Optically thin** to ionizing radiation. Every ionizing photon emitted during the recombination process escapes. For this case, we sum the radiative capture rate coefficient α_{nl} over all levels nl .
 - ▶ **photoionized gas:** Photoionized nebulae around OB stars (H II regions) usually have large enough densities of neutral H. For this situation, case B is an excellent approximation.
 - **Case B: Optically thick** to Lyman continuum and Lyman series. Ionizing photons emitted during recombination are immediately reabsorbed, creating another ion and free electron by photoionization. In this case, the recombinations directly to $n = 1$ do not reduce the ionization of the gas: **only recombinations to $n \geq 2$ act to reduce the ionization.**
 - ▶ **collisionally ionized gas:** Regions where the hydrogen is collisional ionized are typically very hot ($T > 10^6$ K) and have very low density. For these shock-heated regions, case A is an excellent approximation.

Case B

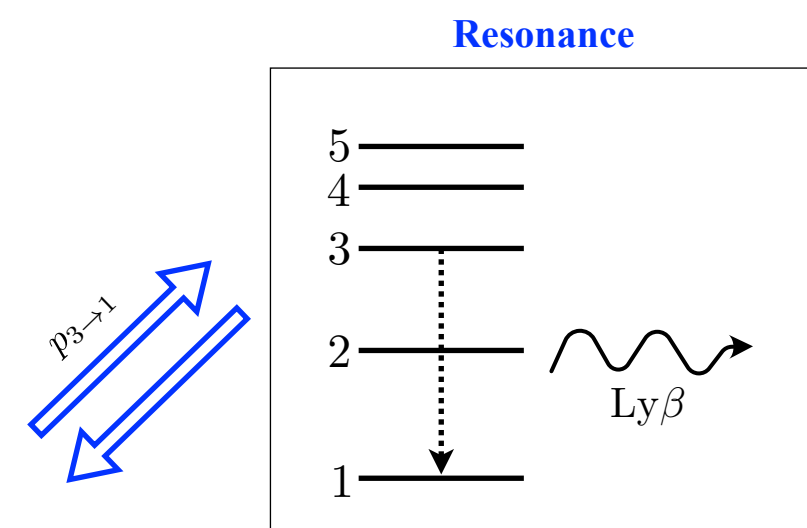
(1) Lyman Continuum Photons



Recombination to $n = 1$



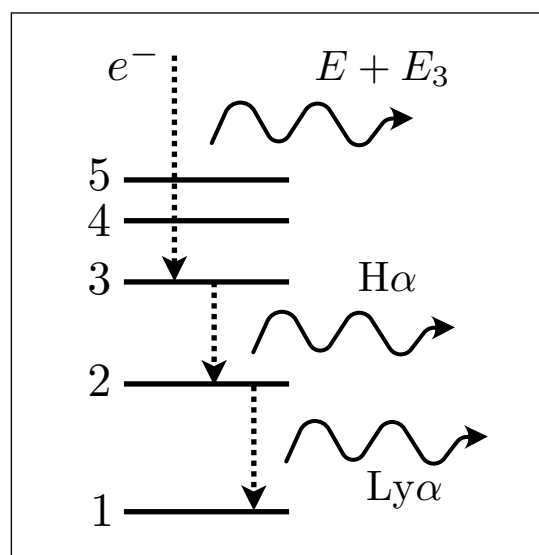
Absorption of emitted LyC photons
by other hydrogen atoms



Resonance

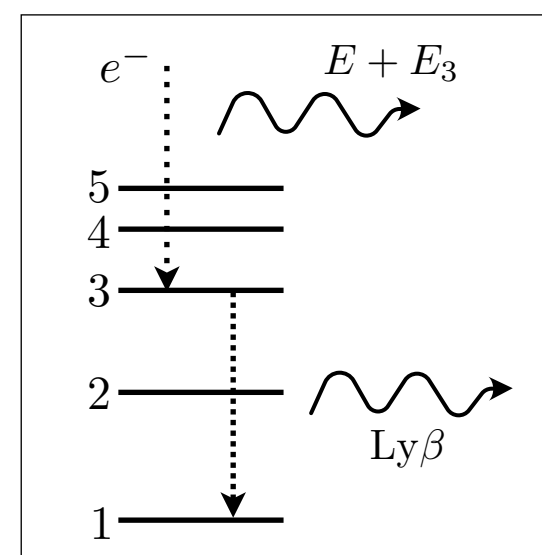
(2) Lyman Series Line Photons

case 1

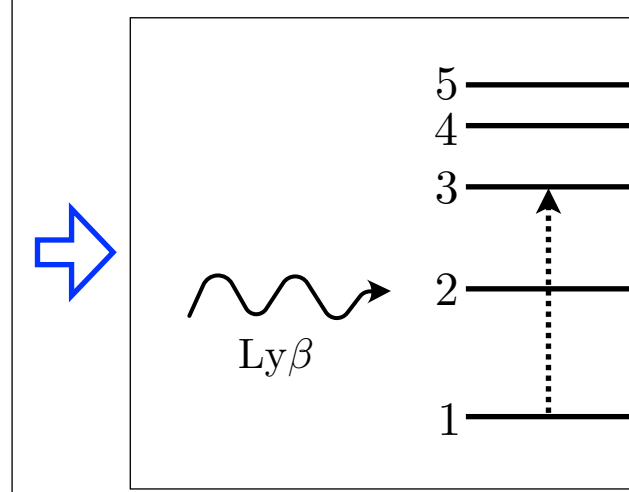


Emission of higher series lines
(Balmer, etc) + Ly α (or 2 photons)

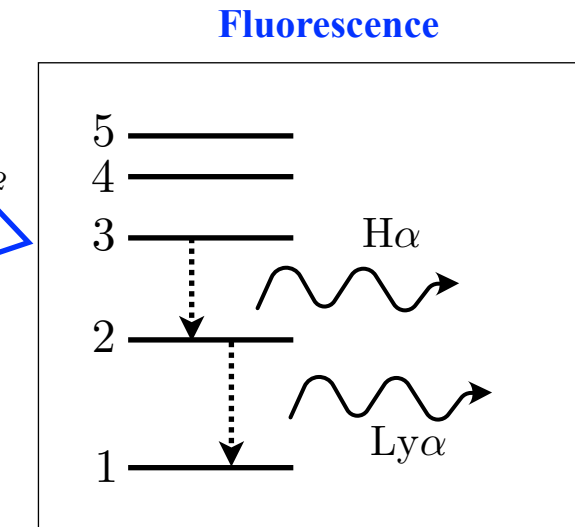
case 2



Emission of Ly n ($n \geq 2$) photons
(Ly β , Ly γ , ...)



Absorption of Ly β photons
by other hydrogen atoms



Fluorescence

H II regions: Photoionization and Recombination of Hydrogen

- ISM, which is primarily composed of hydrogen, is transparent to $h\nu < 13.6$ eV photons, but is very opaque to ionizing photons with $h\nu > 13.6$ eV.
 - Ionized atomic hydrogen regions, broadly termed “H II regions”, are composed of gas ionized by photons with energies above the hydrogen ionization energy of 13.6 eV.



- Sources of ionizing photons include massive, hot young stars, hot white dwarfs, and supernova remnant shocks.

- The photoionization cross-section of H depends strongly on frequency and is reasonably approximated by a power-law:

$$\sigma_{\text{pi}}(\nu) \approx \sigma_0 \left(\frac{h\nu}{I_{\text{H}}} \right)^{-3} \quad \text{for } I_{\text{H}} \lesssim h\nu \lesssim 100I_{\text{H}}$$

$(I_{\text{H}} = 13.6 \text{ eV})$

$$\sigma_0 \equiv \frac{2^9 \pi}{3e^4} \alpha \pi a_0^2 = 6.304 \times 10^{-18} \text{ cm}^2$$

fine-structure constant

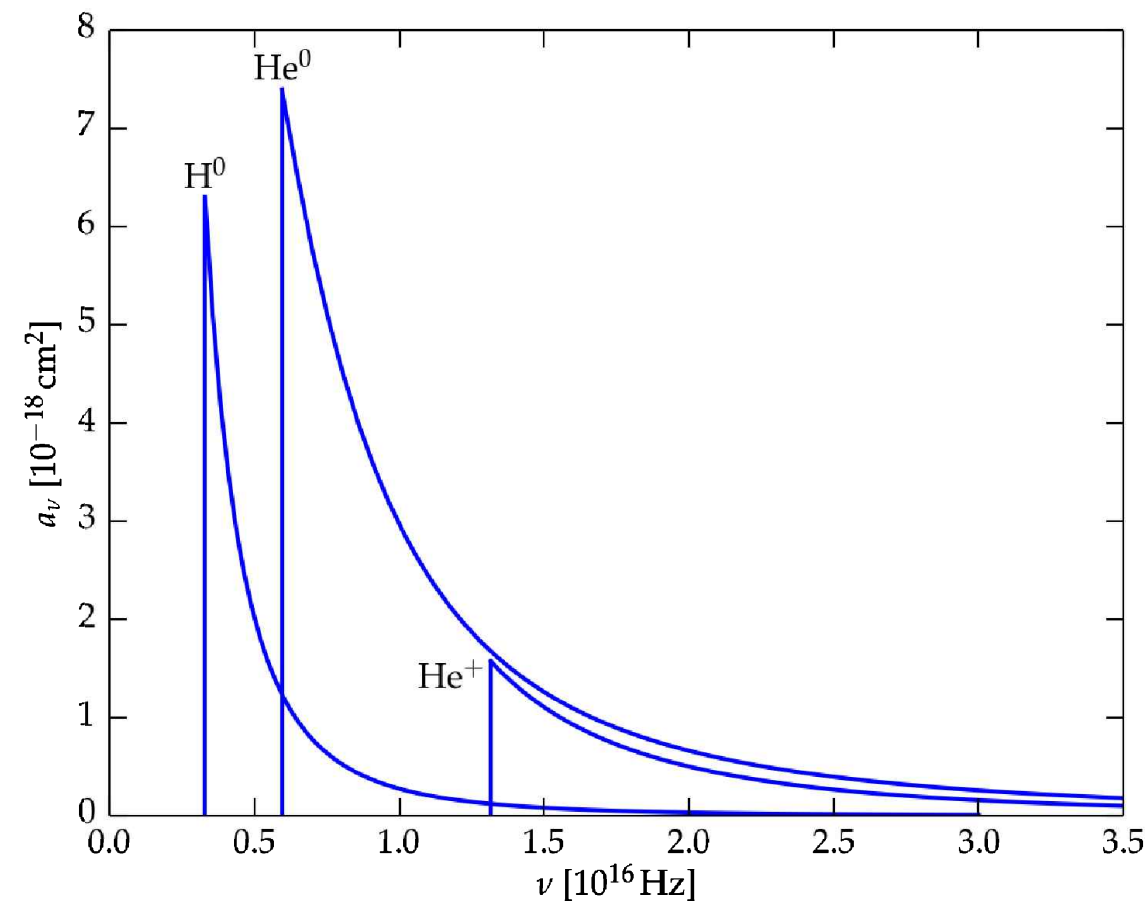
$(\alpha \equiv e^2/hc = 1/137.04, e = 2.71828\dots)$

e = electric charge. e = Euler number

- The recombination rate coefficient (recombination to levels $n \geq 2$) is given in an approximate power law form,

$$\alpha_B(T) \equiv \sum_{n=2}^{\infty} \sum_{\ell=0}^{n-1} \alpha_{n\ell}(T)$$

$$\approx 2.59 \times 10^{-13} T_4^{-0.833 - 0.034 \ln T_4} [\text{cm}^3 \text{s}^{-1}] \quad \text{for } 0.3 \lesssim T_4 = T/10^4 \text{ K} \lesssim 3$$



Photoionization cross section for hydrogen(H^0), hydrogenic helium (He^+), and neutral helium (He^0).
[Fig. 4.1 in Ryden]

The Strömgren Sphere: A Uniform, Pure Hydrogen Nebula

- ***Strömgren Sphere:***
 - Strömgren (1939) considered the simple idealized problem of a fully ionized, spherical region of uniform medium plus a central source of ionizing photons.
 - The ionization is assumed to be maintained by absorption of the ionizing photons radiated by a central hot star. The central source produces ionizing photons (**Lyman continuum; LyC**), with energy $\nu > \nu_0 = I_{\text{H}}/h$ at a constant rate $Q_0 \equiv \dot{N}_{\text{ionize}}$ [photons s⁻¹].
- **O star** temperatures, masses, and ionizing photon rates
 - The emission of the most massive (O-type) stars can be approximated as a blackbody with a peak energy $E \sim 5hc/kT \approx 12.9$ eV, very close to the hydrogen ionization potential.
 - O stars produce enough ionizing photons to create large ionized, or H II, regions.

SpT	T_* (K)	$M_*(M_{\odot})$	$\log_{10}(L_*/L_{\odot})$	$\log_{10}(\dot{N}_{\text{ionize}})$	
O3	44600	58.3	5.83	49.63	LyC $\lambda < 912\text{\AA}$ $E > 13.6\text{ eV}$
O4	43400	46.2	5.68	49.47	
O5	41500	37.3	5.51	49.26	
O6	38200	31.7	5.30	48.96	
O7	35500	26.5	5.10	48.63	
O8	33380	22.0	4.90	48.29	
O9	31500	18.0	4.72	47.90	

- Ionization and Recombination rates:

- Ionization rate per neutral hydrogen atom at a radius $r = 1 \text{ pc}$ from an O star is

$$R_{\text{ionize}} = \frac{\dot{N}_{\text{ionize}}}{4\pi r^2} \sigma_0 \approx 3 \times 10^{-7} \text{ s}^{-1}$$

$\dot{N}_{\text{LyC}} = 5 \times 10^{48} \text{ s}^{-1}$
 $\sigma_0 = 6.3 \times 10^{-18} \text{ cm}^2$
 $r = 1 \text{ pc} = 3.1 \times 10^{18} \text{ cm}$

- This is much greater than the recombination rate per hydrogen ion,

$$R_{\text{recombine}} = \alpha_B n_e \approx 3 \times 10^{-12} \left(\frac{n_e}{10 \text{ cm}^{-3}} \right) \text{ s}^{-1} \quad \text{at } T = 10^4 \text{ K}$$

- This implies a neutral hydrogen atom near the center of the nebula would survive a few months before being ionized but then, once ionized, would **have to wait about ten thousand years before recombining with a free electron**. We conclude that, at 1 pc, the nebula is almost fully ionized.
- As we move outwards in the nebula away from the O star the ionization rate decreases as $1/r^2$ and eventually will match the recombination rate. This defines the boundary of the H II region.

-
- The transition from ionized to neutral will occur at a length scale of the mean free path of photoionization in the neutral gas.

$$\lambda_{\text{mfp}} = \frac{1}{n_{\text{H}} \sigma_{\text{pi}}} \sim 5 \times 10^{-4} \text{ pc} \left(\frac{n_{\text{H}}}{10^2 \text{ cm}^{-3}} \right)^{-1} \left(\frac{\sigma_{\text{pi}}}{6.304 \times 10^{-18} \text{ cm}^2} \right)^{-1}$$

- This length scale is over a thousand times smaller than the observed size of the nebula.
- Therefore, the gas is either fully ionized or neutral.
- This tells us that the transition from ionized gas to neutral gas at the boundary of the H II region will occur over a distance that is very small compared to the Strömgren radius.

- Assuming that ***the ionization is nearly complete ($n_p = n_e = n_H$) within R_s*** , and nearly zero ($n_{H^0} = n_H, n_e = 0$) outside R_s , we obtain the size of the ionized region by simply equating the rate of ionization to the rate of recombination (over the whole volume of the ionized region):

$$Q_0 = (n_H^2 \alpha_B) \frac{4\pi}{3} R_s^3 \quad \longleftarrow \quad Q_0 = \dot{N}_{LyC}$$

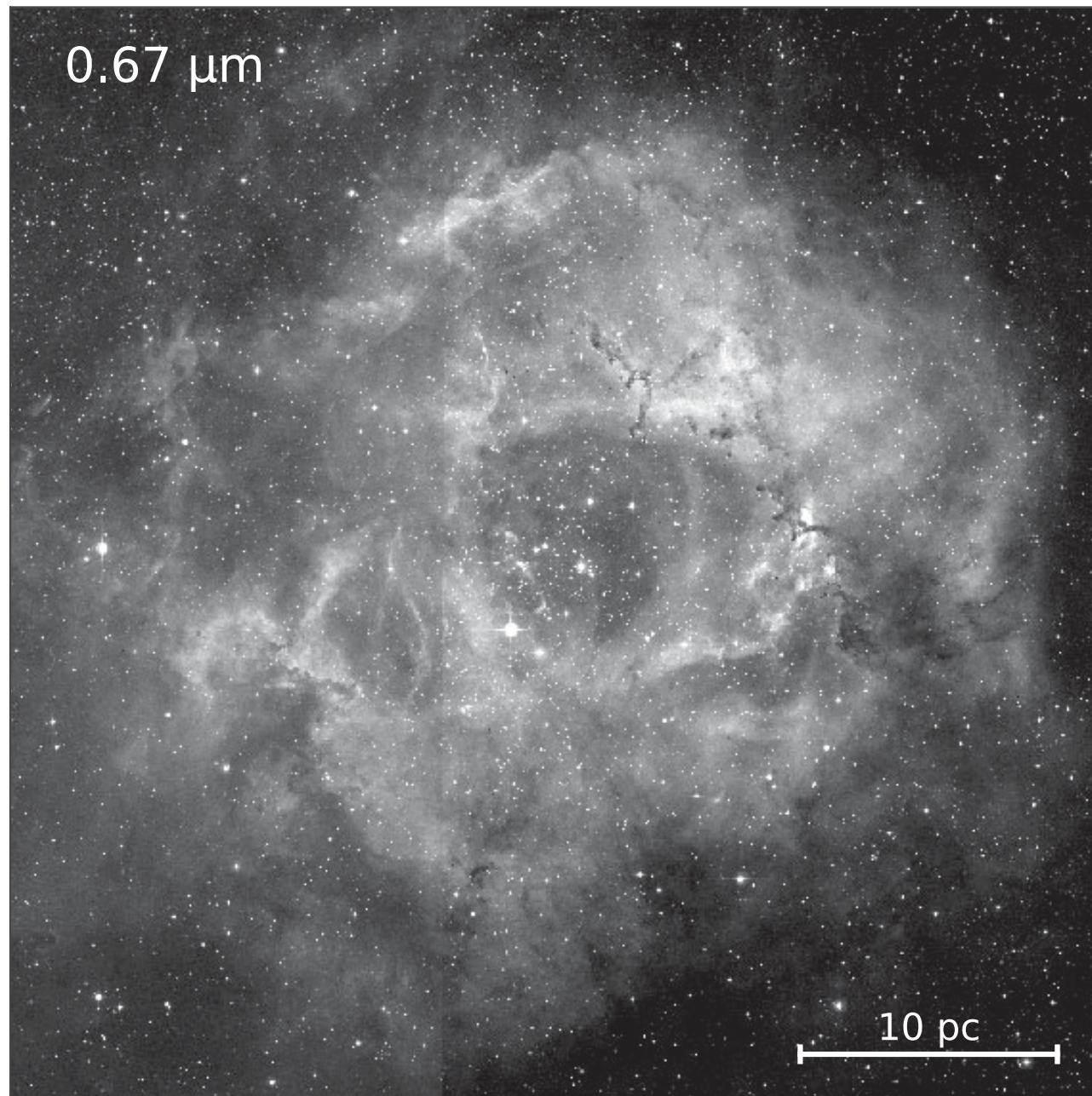
- This gives the Strömgren radius:

$$\begin{aligned} R_s &= \left(\frac{3}{4\pi} \frac{Q_0}{\alpha_B n_H^2} \right)^{1/3} \\ &= 3.17 \left(\frac{Q_0}{10^{49} \text{ photons s}^{-1}} \right)^{1/3} \left(\frac{n_H}{10^2 \text{ cm}^{-3}} \right)^{-2/3} \left(\frac{T}{10^4 \text{ K}} \right)^{0.28} \text{ [pc]} \end{aligned}$$

The physical meaning of this is that ***the total number of ionizing photons emitted by the star balances the total number of recombinations within the ionized volume*** $(4\pi/3)R_s^3$, often called the Strömgren sphere. Its radius R_s is called the Strömgren radius.

H II region - Rosette nebula

- For the Rosette, we find the theoretical size to be $R_S = 40$ pc which is about a factor of 2 larger than its observed extent. **The discrepancy is because some of the ionizing photons are absorbed by dust.**

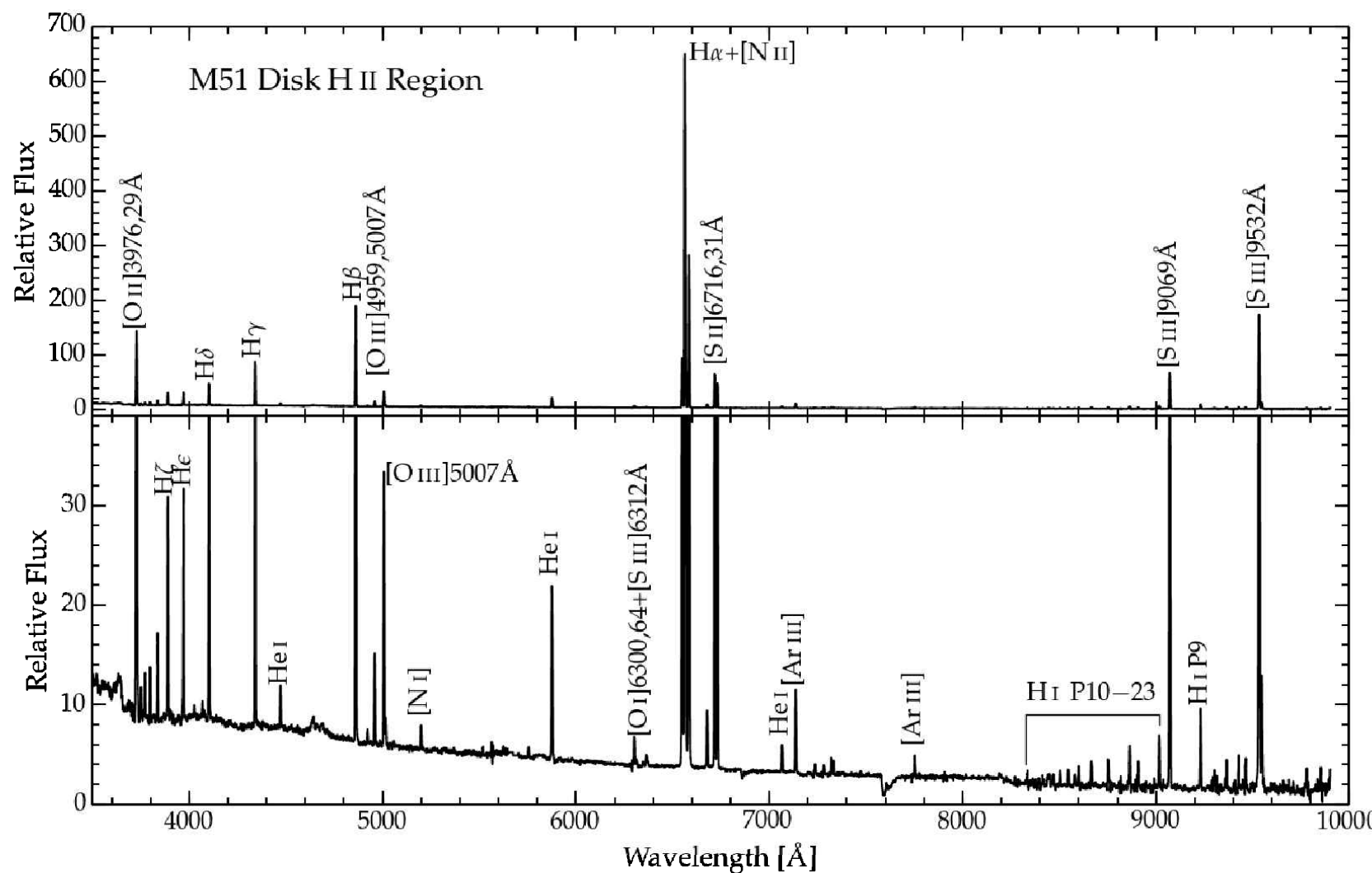


Optical (DSS2 Red) image of the Rosette nebula.

[Fig 6.1, J. P. Williams]

Nebular Emission Lines

- In the figure, the continuum is a mixture of **free-bound continuum** (from radiative recombination), **free-free emission** (thermal bremsstrahlung), and **two-photon emission**.
- The ***collisionally excited emission lines*** are much stronger than the continuum spectrum. The collisional emission lines are utilized to measure the temperature and density of the medium.



Spectrum of a disk HII region in the Whirlpool galaxy (M51).

(top) bright lines

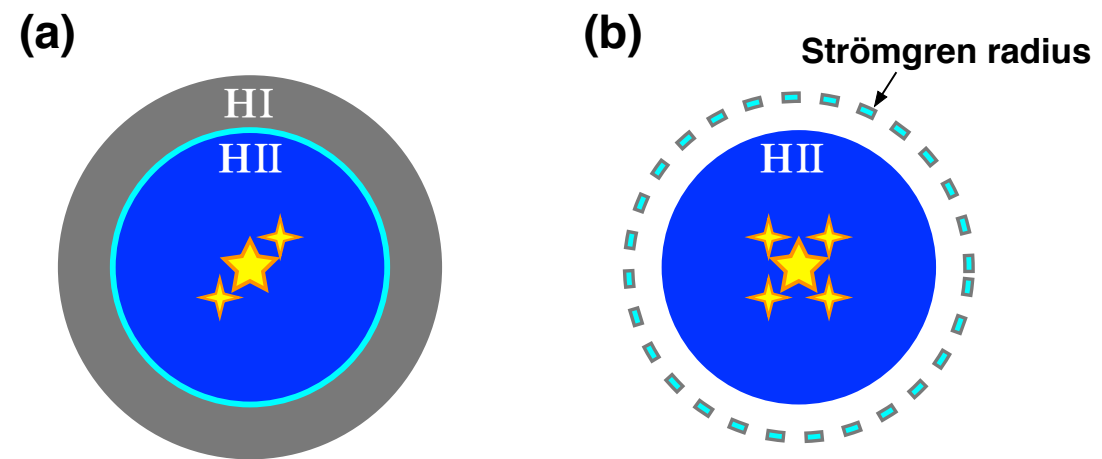
(bottom) scaled to show faint lines.

Figure 4.6 [Ryden]

Properties of Ionized Hydrogen Regions

- Ionized atomic hydrogen regions, broadly termed “H II regions”, are composed of gas ionized by photons with energies above the hydrogen ionization energy of 13.6 eV.
 - Ionization Bounded:** These objects include “*classical H II regions*” ionized by hot O or B stars (or clusters of such stars) and associated with regions of recent massive-star formation, and “planetary nebulae”, the ejected outer envelopes of AGB stars photoionized by the hot remnant stellar core.
 - Density Bounded: Warm Ionized Medium / Diffuse Ionized Gas:** Ionized Gas in the diffuse ISM, far away from OB associations.

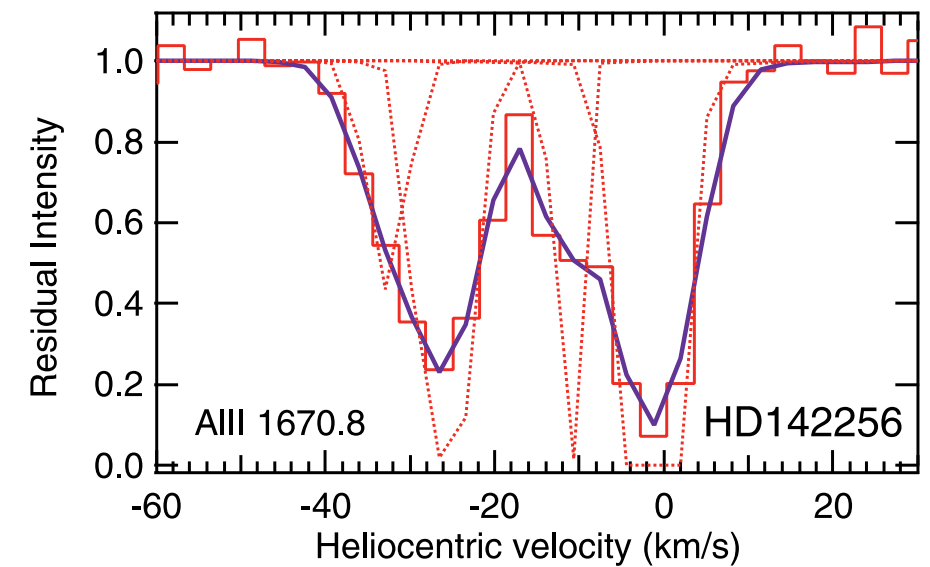
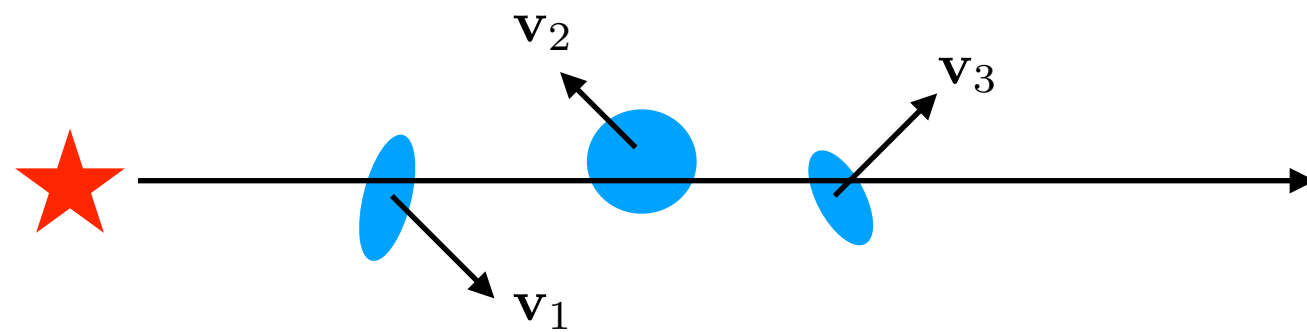
- (a) An ionization-bounded nebula whose radius is determined by the ionization equilibrium. The **LyC is entirely consumed** to ionized the surrounding H I gas.
- (b) In a density-bounded nebula, the amount of the surrounding H I gas is not enough to consume all LyC photons. Some of the **LyC escapes** from the cloud, which is called the LyC leakage.



- Two important processes governing the physics of H II regions:
 - Photoionization Equilibrium:** the balance between photoionization and recombination. This determines the spatial distribution of ionic states of the elements in the ionized zone.
 - Thermal Balance** between heating and cooling. Heating is dominated by photoelectrons ejected from hydrogen and helium with thermal energies of a few eV. Cooling is mostly dominated by electron-ion impact excitation of metal ion followed by emission of “forbidden” lines from low-lying fine structure levels. It is these cooling lines that give H II regions their characteristic spectra.

<Absorption Lines> Observations of Metallic Absorption Lines Toward the CNM

- The composition and excitation of interstellar gas can be studied using absorption lines that appear in the spectra of background stars (or other sources).
 - The most prominent absorption lines at visible wavelengths are Ca II K and H lines at $\lambda = 3933, 3968 \text{ \AA}$, and Na I D₁ and D₂ doublet lines at $\lambda = 5890, 5896 \text{ \AA}$.
- Absorption lines (and emission lines) contains information about number density, temperature, chemical abundances, ionization states, and excitation states.
 - However, interpreting the information requires understanding the ways in which light interacts with baryonic matter, radiative transfer.
 - We need to know the line profile to analyze absorption lines.**



- **The interstellar absorption lines are typically narrow** compared to spectral features produced by absorption in stellar photospheres, and in practice can be readily distinguished.
- **It is normally possible to detect absorption only by the ground state** (and perhaps the excited fine-structure levels of the ground electronic state) - the populations in the excited electronic states are too small to be detected in absorption.
- The widths of absorption lines are usually determined by Doppler broadening, with line widths of a few km s⁻¹ (or $\Delta\lambda/\lambda \approx 10^{-5}$) - often observed in cool clouds.
- However, interpreting the information requires understanding the ways in which light interacts with baryonic matter, radiative transfer.
- **We need to know the line profile to analyze absorption lines.**

Line Broadening Mechanisms

- ***Atomic levels are not infinitely sharp***, nor are the lines connecting them.
 - (1) Doppler (Thermal) Broadening
 - (2) Natural Broadening
 - (3) Collisional Broadening
 - (4) Thermal Doppler + Natural Broadening
- **Voigt profile : Thermal + Natural broadening**
 - Atoms shows both a Lorentz profile plus the Doppler effect.
 - In this case, we can write the profile as an average of the Lorentz profile over the various velocity states of the atom:
 - ***Voigt profile = convolution of a Lorentz function (natural broadening) and Gaussian function (thermal broadening).***

Intrinsic Absorption & Emission Line Profile

- In the classical / quantum theory of spectral lines,**

we obtain a Lorentzian line profile:

$$\sigma_\nu = f_{nn'} \frac{\pi e^2}{m_e c} \frac{\gamma/4\pi^2}{(\nu - \nu_0)^2 + (\gamma/4\pi)^2}$$

$$\int_0^\infty \sigma_\nu d\nu = f_{nn'} \frac{\pi e^2}{m_e c}$$

m_e = electron mass
 e = electric charge

where $f_{nn'}$ is called the **oscillator strength** or **f-value** for the transition between states n and n' .

$\gamma = A$ is the **damping constant (or Einstein A-coefficient)**.

Note that the intrinsic line profiles of the absorption and emission lines are the same.

Selected Resonance Lines^a with $\lambda < 3000 \text{ \AA}$

	Configurations	ℓ	u	$E_\ell/hc(\text{cm}^{-1})$	$\lambda_{\text{vac}}(\text{\AA})$	$f_{\ell u}$
C IV	$1s^2 2s - 1s^2 2p$	$^2S_{1/2}$	$^2P_{1/2}^o$	0	1550.772	0.0962
		$^2S_{1/2}$	$^2P_{3/2}^o$	0	1548.202	0.190
N V	$1s^2 2s - 1s^2 2p$	$^2S_{1/2}$	$^2P_{1/2}^o$	0	1242.804	0.0780
		$^2S_{1/2}$	$^2P_{3/2}^o$	0	1242.821	0.156
O VI	$1s^2 2s - 1s^2 2p$	$^2S_{1/2}$	$^2P_{1/2}^o$	0	1037.613	0.066
		$^2S_{1/2}$	$^2P_{3/2}^o$	0	1037.921	0.133
C III	$2s^2 - 2s 2p$	1S_0	$^1P_1^o$	0	977.02	0.7586
C II	$2s^2 2p - 2s 2p^2$	$^2P_{1/2}^o$	$^2D_{3/2}^o$	0	1334.532	0.127
		$^2P_{3/2}^o$	$^2D_{5/2}^o$	63.42	1335.708	0.114
N III	$2s^2 2p - 2s 2p^2$	$^2P_{1/2}^o$	$^2D_{3/2}^o$	0	989.790	0.123
		$^2P_{3/2}^o$	$^2D_{5/2}^o$	174.4	991.577	0.110
CI	$2s^2 2p^2 - 2s^2 2p 3s$	3P_0	$^3P_1^o$	0	1656.928	0.140
		3P_1	$^3P_2^o$	16.40	1656.267	0.0588
		3P_2	$^3P_2^o$	43.40	1657.008	0.104
N II	$2s^2 2p^2 - 2s 2p^3$	3P_0	$^3D_1^o$	0	1083.990	0.115
		3P_1	$^3D_2^o$	48.7	1084.580	0.0861
		3P_2	$^3D_3^o$	130.8	1085.701	0.0957
N I	$2s^2 2p^3 - 2s^2 2p^2 3s$	$^4S_{3/2}^o$	$^4P_{5/2}$	0	1199.550	0.130
		$^4S_{3/2}^o$	$^4P_{3/2}$	0	1200.223	0.0862
O I	$2s^2 2p^4 - 2s^2 2p^3 3s$	3P_2	$^3S_1^o$	0	1302.168	0.0520
		3P_1	$^3S_1^o$	158.265	1304.858	0.0518
		3P_0	$^3S_1^o$	226.977	1306.029	0.0519
Mg II	$2p^6 3s - 2p^6 3p$	$^2S_{1/2}$	$^2P_{1/2}^o$	0	2803.531	0.303
		$^2S_{1/2}$	$^2P_{3/2}^o$	0	2796.352	0.608
Al III	$2p^6 3s - 2p^6 3p$	$^2S_{1/2}$	$^2P_{1/2}^o$	0	1862.790	0.277
		$^2S_{1/2}$	$^2P_{3/2}^o$	0	1854.716	0.557

Table 9.4 in [Draine]

See also Table 9.3

- The profile can be written using the Voigt function.

$$\phi(\nu) = \frac{1}{\Delta\nu_D \sqrt{\pi}} H(u, a)$$

$$H(0, a) \approx 1$$

$$\phi(\nu = 0) \approx \frac{1}{\Delta\nu_D \sqrt{\pi}}$$

Here, Voigt function is defined as

$$H(u, a) \equiv \frac{a}{\pi} \int_{-\infty}^{\infty} \frac{e^{-y^2} dy}{(u - y)^2 + a^2}$$

$$a \equiv \frac{\Gamma}{4\pi\Delta\nu_D}$$

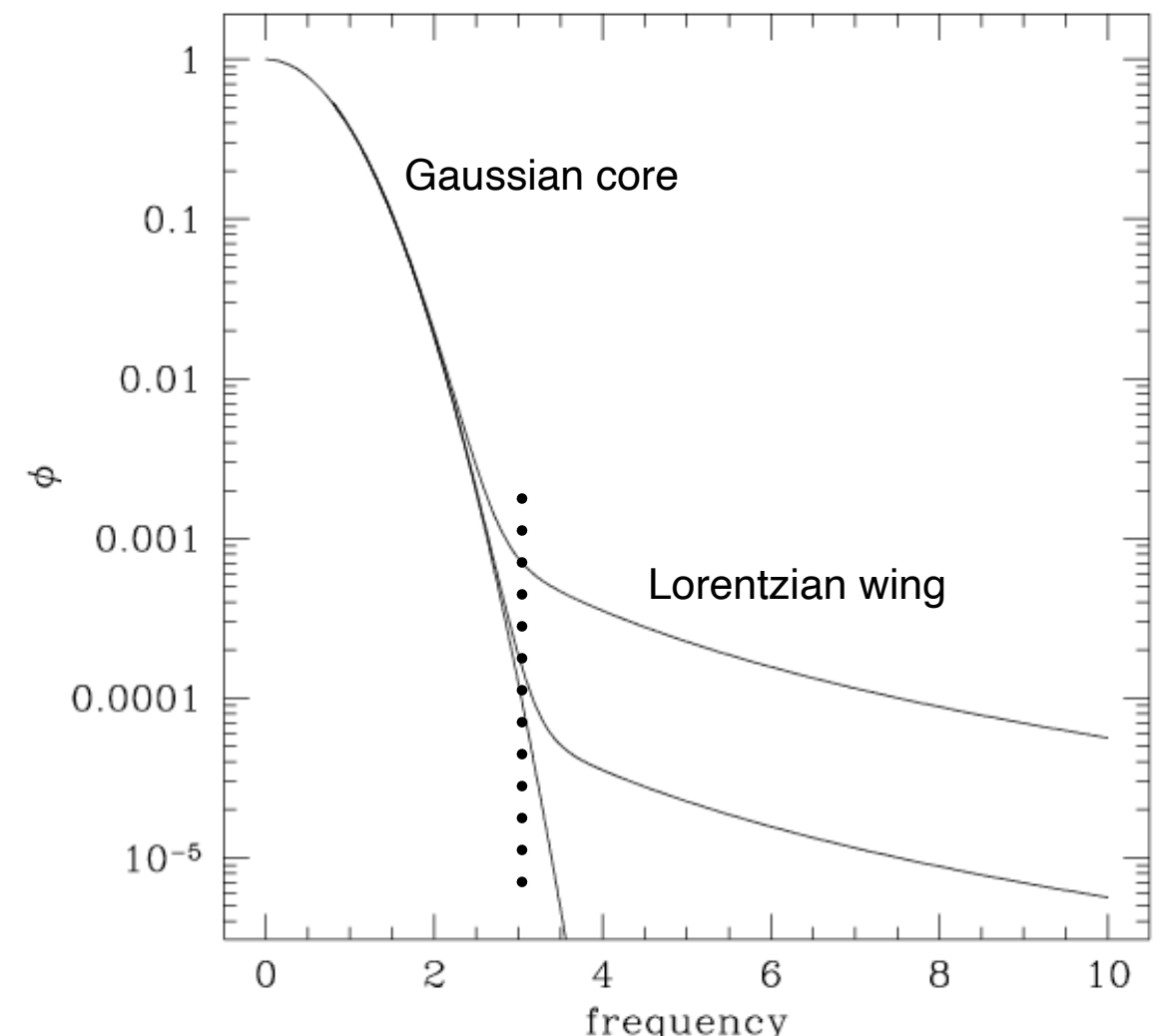
$$u \equiv \frac{\nu - \nu_0}{\Delta\nu_D}$$

Thermal Doppler broadening parameter:

$$\Delta\nu_D = \nu_0 \frac{v_{\text{th}}}{c} = \frac{\nu_0}{c} \sqrt{\frac{2kT}{m}} = \frac{v_{\text{th}}}{\lambda_0}$$

Here, a is a ratio of the intrinsic broadening Γ to the thermal broadening $\Delta\nu_D$.

u is a measure of how far you are from the line center, in units of thermal broadening parameter.



Including the turbulent motion, the Doppler parameter is

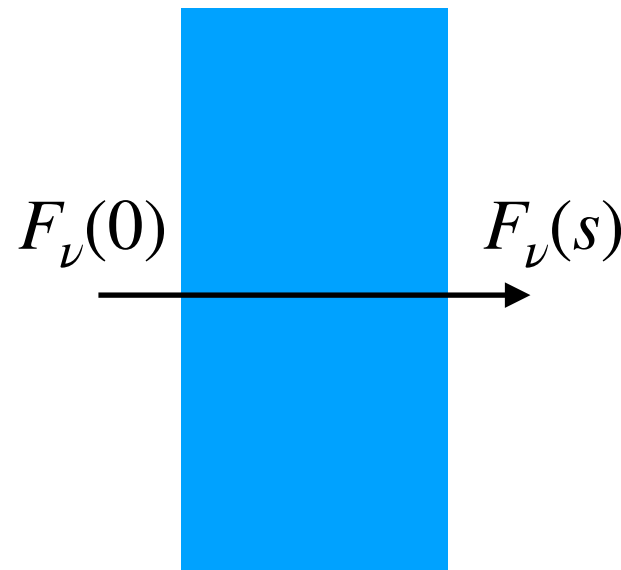
$$\Delta\nu_D = \nu_0 \frac{v_{\text{th}}}{c} \rightarrow \Delta\nu_D = \nu_0 \frac{b}{c} = \frac{b}{\lambda_0}$$

$$\text{where } b = \sqrt{v_{\text{th}}^2 + v_{\text{turb}}^2}, \quad v_{\text{th}} = \sqrt{\frac{2kT}{m}}$$

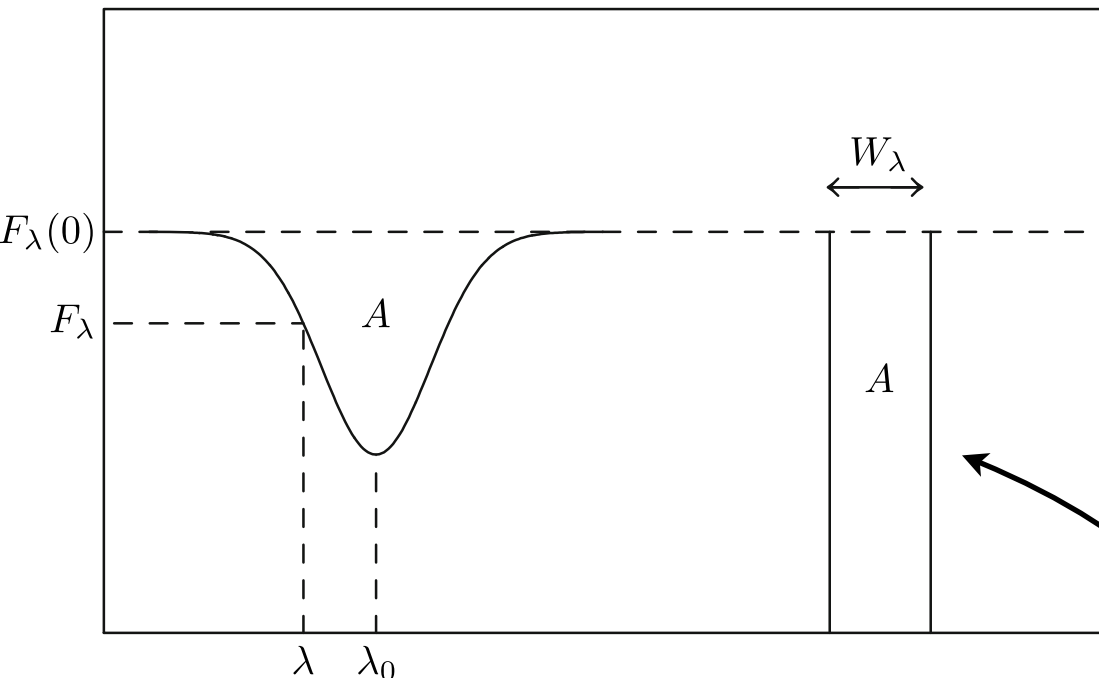
v_{turb} is the rms velocity of the turbulent motion.

**Thermal velocity depends on the atom's mass.
However, turbulent velocity is independent of the mass.**

Absorption Line & Equivalent Width



$$F_\nu = F_\nu(0)e^{-\tau_\nu}$$



$$\tau_\nu = \tau_0 H(u, a)$$

$$\tau_0 = \frac{\sqrt{\pi}e^2}{m_e c} f_{\ell u} \frac{\lambda_{\ell u}}{b} N_\ell$$

Here, τ_0 is the optical depth at the line center.
 N_ℓ is the column density of the atoms in the lower (ground) level.

Cross section at line center : $\sigma_0 = \frac{\pi e^2}{m_e c} f_{\ell u} \phi(\nu = 0) = \frac{\pi e^2}{m_e c} f_{\ell u} \frac{\lambda_{\ell u}}{\sqrt{\pi b}}$

(wavelength) equivalent width

- **Equivalent width**

$$W_\lambda \equiv \int d\lambda \left[1 - \frac{F_\lambda}{F_\lambda(0)} \right] = \int d\lambda (1 - e^{-\tau_\lambda})$$

- The spectrograph often lack the spectral resolution to resolve the profiles of narrow lines, but can measure the total amount of “missing power” resulting from a narrow absorption line.
- *The equivalent width is the width of a straight-sided, perfectly black absorption line that has the same integrated flux deficit as the actual absorption line.*

Variation of Line Profiles & Curve of growth

- ***The absorption line profiles for $b = 10 \text{ km s}^{-1}$***

- When $\tau_0 < 1$, $F_\nu/F_\nu(0) \approx 1 - \tau_\nu$ and thus the shape of an absorption line resembles an **upside-down Voigt function**.
- When $\tau_0 \gg 1$, the absorption line saturates at its center and becomes increasingly “**box-shaped**.”

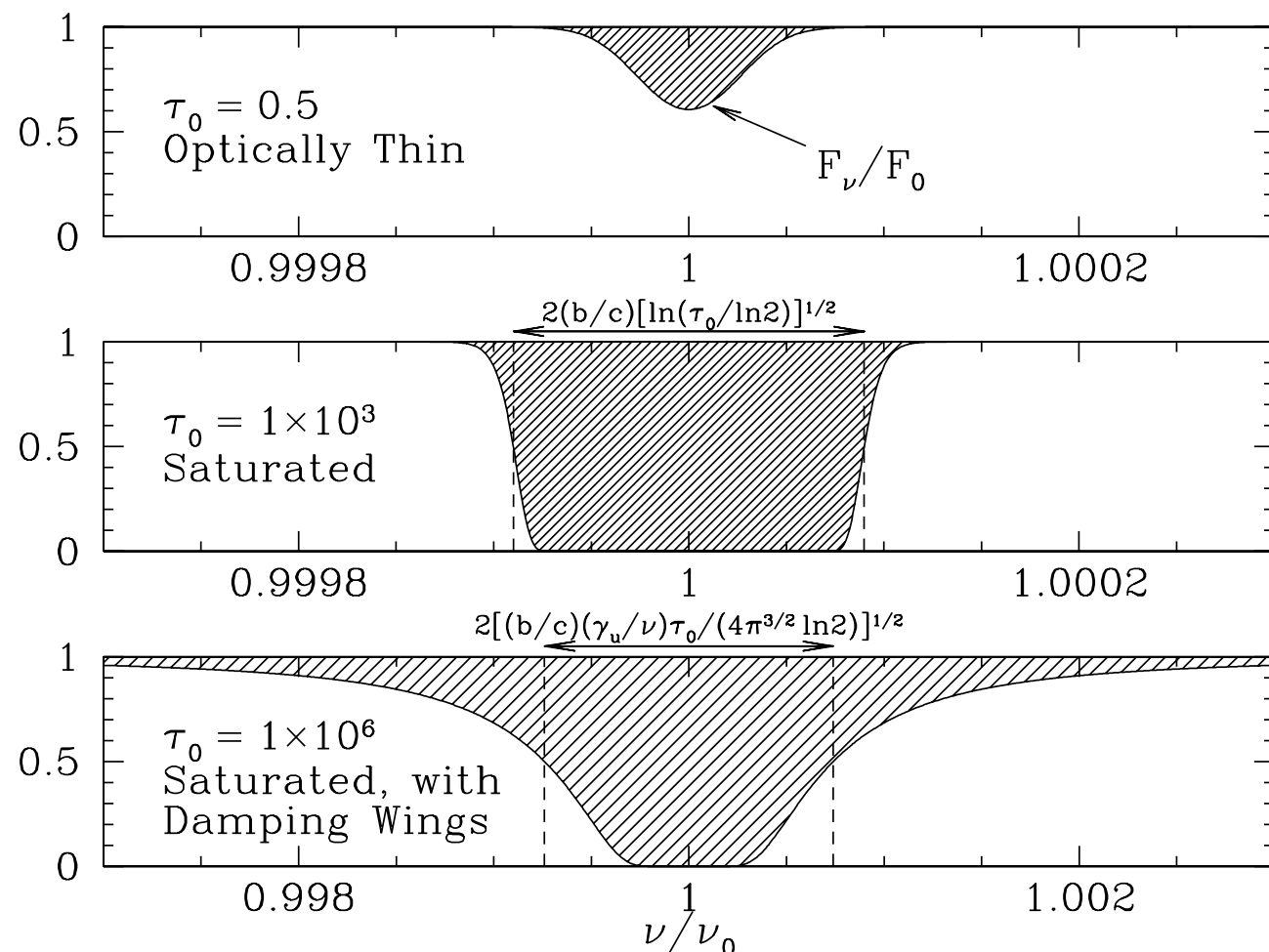
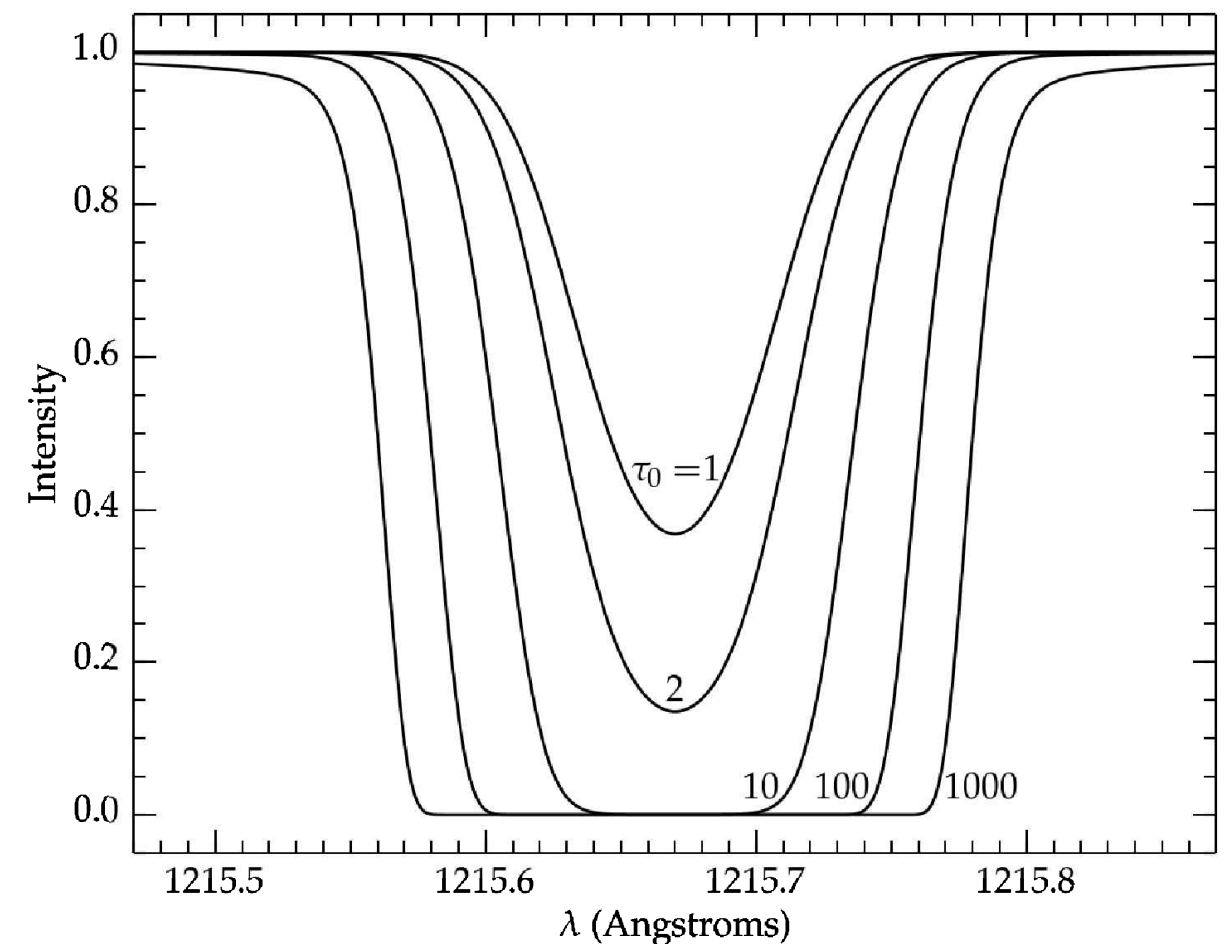


Figure 9.1 in [Draine]

Note the different abscissa in the lowest panel.



Lyman α absorption lines for $b = 10 \text{ km s}^{-1}$.

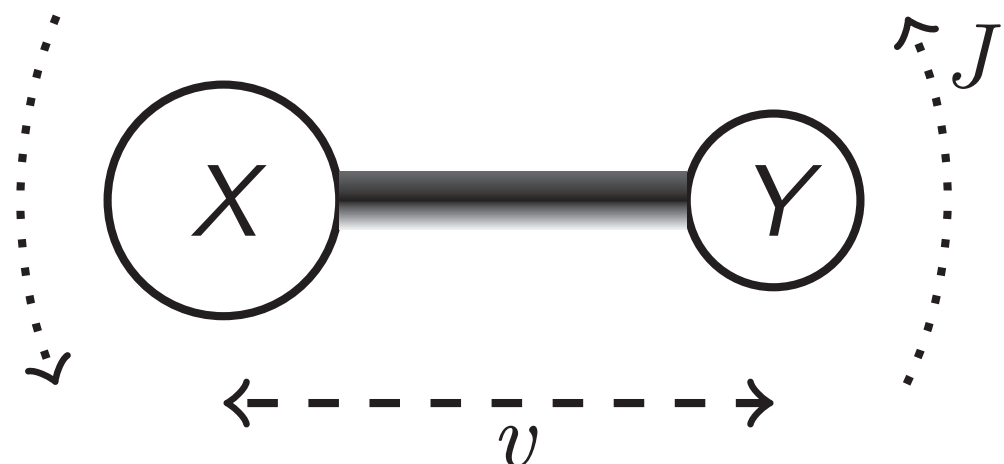
Figure 2.6 in [Ryden]

- ***Curve of growth***

- The curve of growth refers to the relation between the observed equivalent width and the underlying optical depth (or the column density) of the absorber.

Molecular Clouds

- In dense regions (away from energetic sources of radiation), atoms can combine to form molecules.
 - **Electronic states:** The electrons share orbitals around two or more nuclei with transitions that produce UV and optical lines analogous to those in atoms.
 - **Vibrational and rotational states:** In addition, the interactions of the nuclei themselves have quantized vibrational and rotational states, though at much lower energies. The corresponding lines lie in the IR and mm wavelength regime.



Schematic of the vibrational and rotational modes of a diatomic molecule, with quantum numbers v and J respectively.

- Classically, the vibration and rotation can be viewed as an accelerating charge.
- Observations reveal a rich spectrum from multiple species that tells us about the physical and chemical properties of the molecular ISM, which is the coldest parts of the Universe and the sites of stellar birth.

Molecular Structure: Bohn-Oppenheimer Approximation

- **Bohn-Oppenheimer approximation:**

- The motions of the electrons and nuclei could be treated separately.

This come about because of the great difference between the masses of the electron and a typical nuclei.

- The slowly moving nuclei only sense the electrons as a kind of smoothed-out cloud. As the nuclei move, **the electrons have sufficient time to adjust to adiabatically the new nuclear positions.** The nuclei then feel only an equivalent potential that depends on the internuclear distance and on the particular electronic state.
 - Due to very different energies of the **electronic, vibrational, and rotational states**, these interactions can be assumed to be decoupled. The separation of wavefunctions is referred to as the Born-Oppenheimer approximation. Under the Born-Oppenheimer approximation, the total wavefunction is a product of the nuclear, electronic, vibrational, and rotational wavefunctions.

$$\psi_{\text{tot}} = \psi_{\text{nuc}} \psi_{\text{el}} \psi_{\text{vib}} \psi_{\text{rot}}$$

Order of magnitude of energy levels

- Energy Levels

$$E_{\text{elect}} : E_{\text{vib}} : E_{\text{rot}} = 1 : \left(\frac{m_e}{M}\right)^{1/2} : \left(\frac{m_e}{M}\right)$$

- Since $M \approx 10^4 m_e$ ($m_p/m_e = 1836$), the relative strengths of electronic, vibrational, and rotational transitions are

$$E_{\text{elect}} : E_{\text{vib}} : E_{\text{rot}} \sim 1 : 10^{-2} : 10^{-4}$$

- Typical values are

$$E_{\text{elect}} : E_{\text{vib}} : E_{\text{rot}} \sim 10 \text{ eV} : 0.1 \text{ eV} : 0.001 \text{ eV}$$

UV IR IR or radio

- Typical wavelengths are

$$\lambda_{\text{elect}} : \lambda_{\text{vib}} : \lambda_{\text{rot}} \sim 100 \text{ nm} : 10 \mu\text{m} : 1 \text{ mm}$$

- That is, electronic transitions are in the optical/ultraviolet, vibrational in the near/mid-infrared, and rotational in the (sub-)millimeter.

[Energy Levels, Pure rotational & ro-vibrational transitions]

- **Energy Levels**

$$E_q(v, J) = V_q(r_0) + h\nu_0 \left(v + \frac{1}{2} \right) + B_v J(J+1)$$

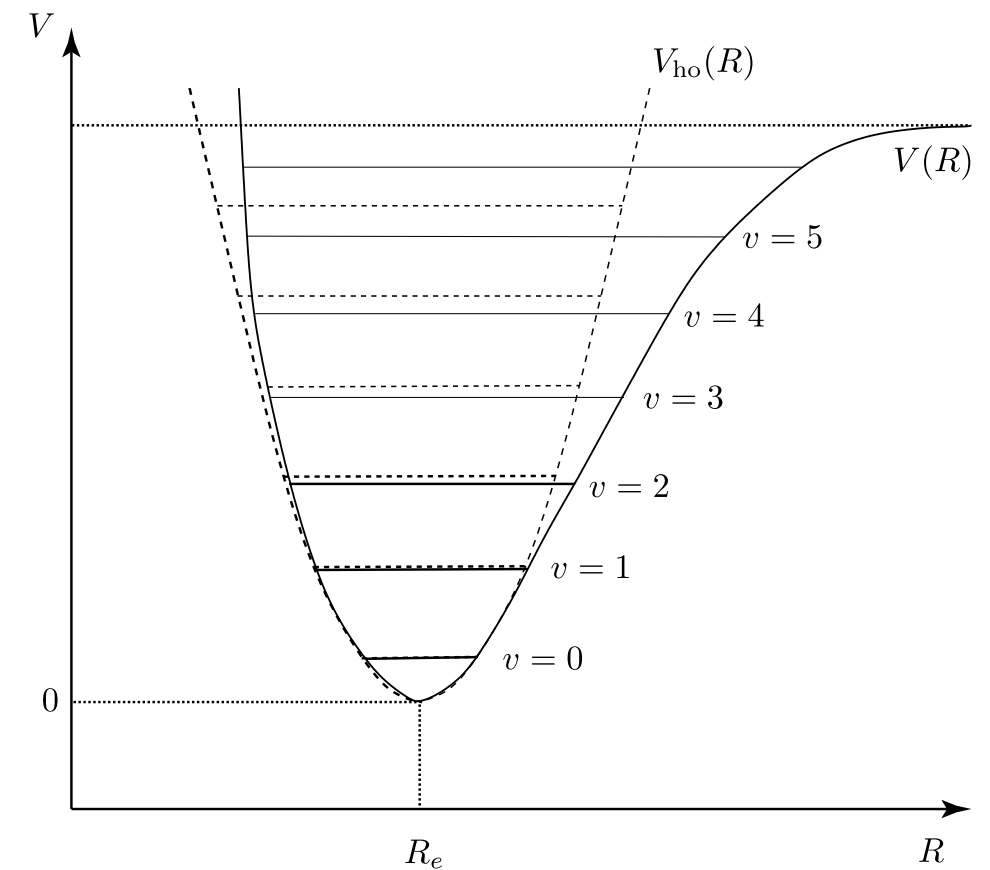
$$\begin{aligned} v &= 0, 1, 2, \dots \\ J &= 0, 1, 2, \dots \end{aligned}$$

$$\nu_0 \equiv \frac{\omega_0}{2\pi} \quad B_v = \frac{\hbar^2}{2I} \quad I = \mu r_0^2 \quad = \text{moment of inertia of the molecule.}$$

Here, q denotes an electronic state.

- **Pure rotational spectrum:** In the lowest vibrational and electronic states, it is possible to have transitions solely among the rotational states. Such transitions give rise to a pure rotational spectrum.
- **Rotational-vibration spectrum:** Because the energies required to excite vibrational modes are much larger than those required to excite rotation, it is unlikely to have a pure vibrational spectrum.

The transitions then yield a rotation-vibrational spectrum, in which both the vibrational state and the rotational state can change together.



[Selection Rules]

- Electric-dipole selection rule for the ro-vibrational transitions:

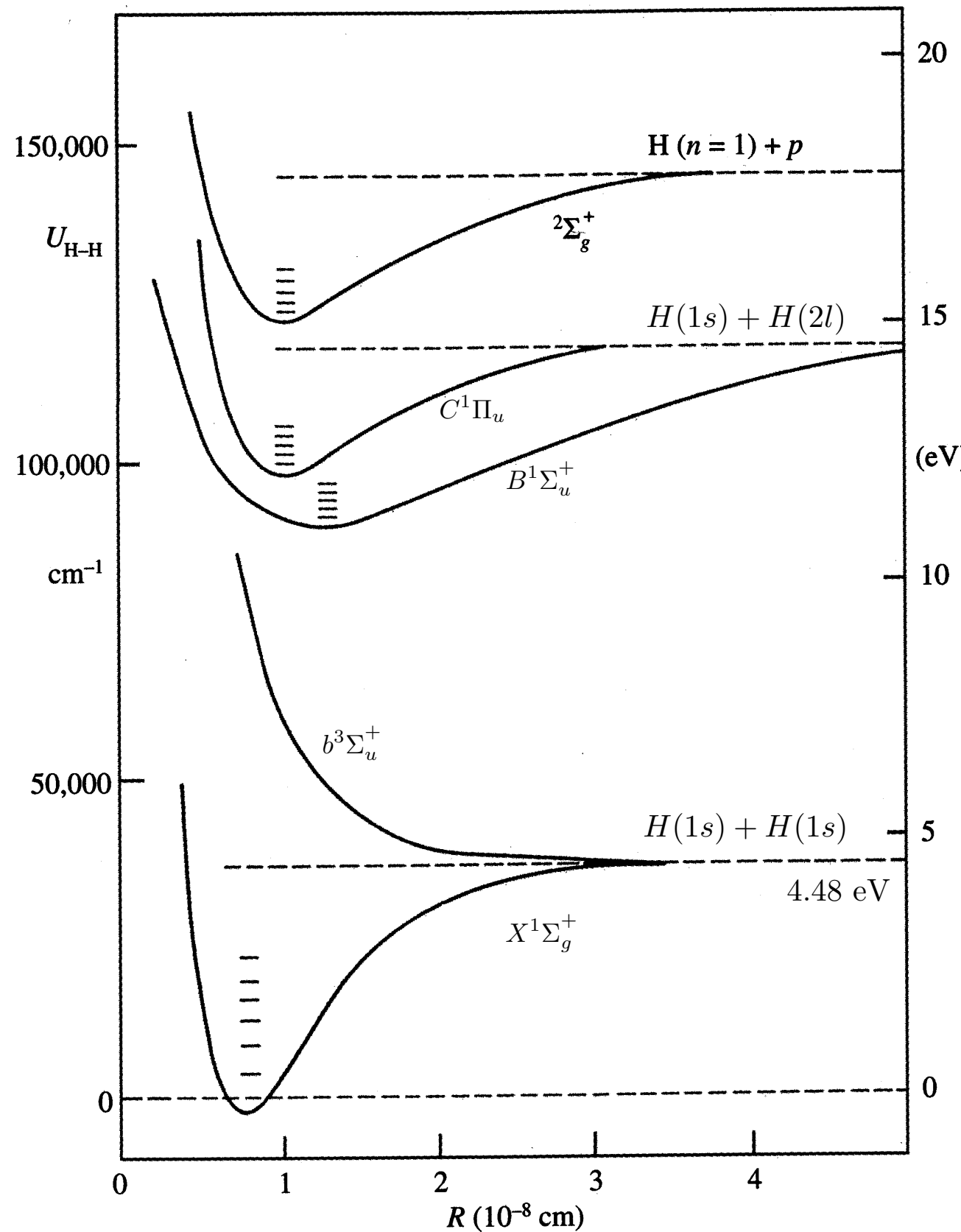
$$\Delta v = \text{any}$$

$$\Delta J = 0, \pm 1 \quad \text{not} \quad J = 0 \leftrightarrow 0$$

- But, note that H₂ has no permanent electric-dipole moment.

The electric-quadrupole are allowed for $\Delta J = \pm 2$ within the ground electronic state.

[Energy levels of Molecular Hydrogen]

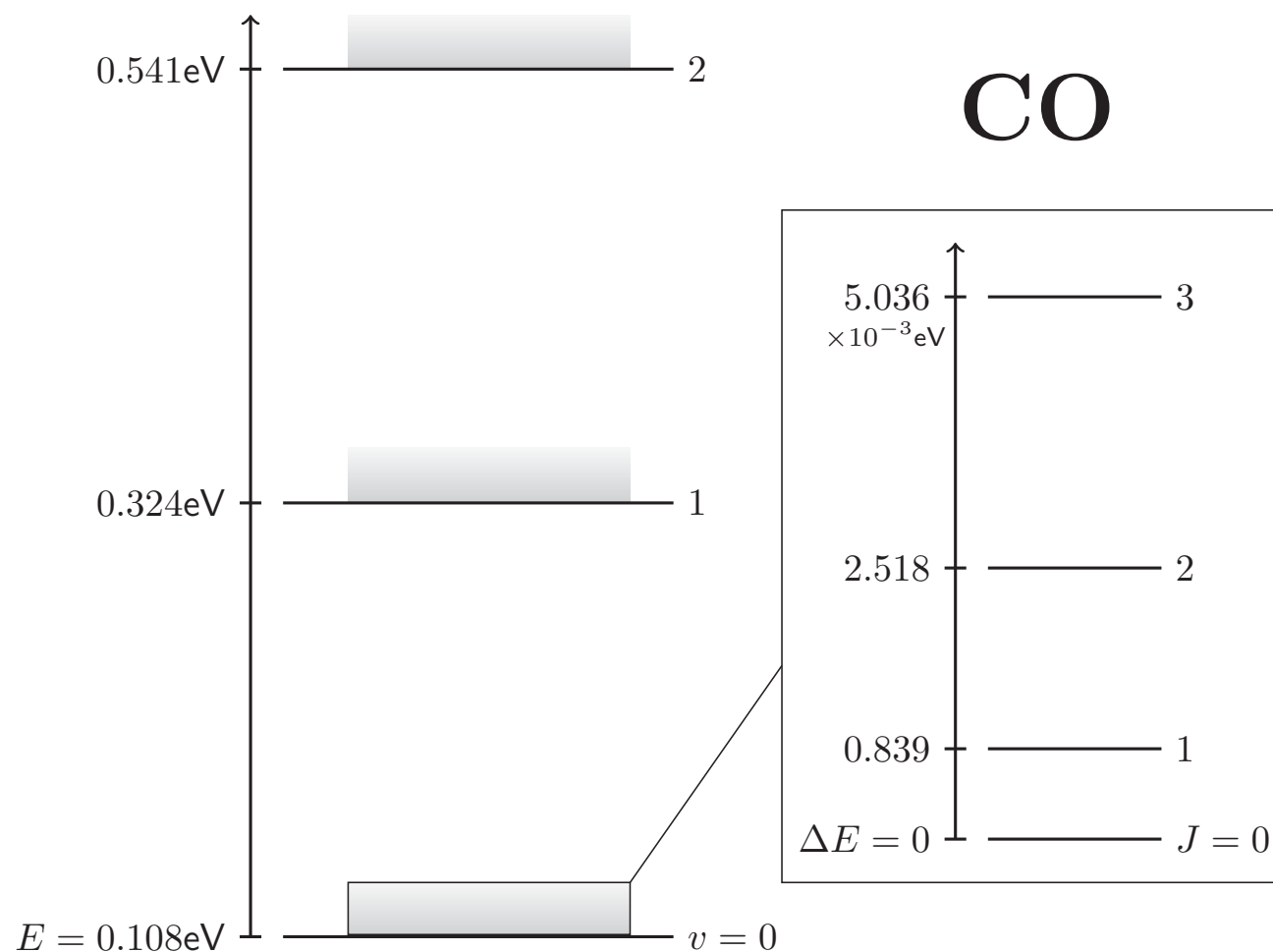


- The short horizontal lines in each of the bound states indicate the vibrational levels.
- The transition from the ground state $X^1\Sigma_g^+$ to the excited states $B^1\Sigma_u^+$ and $C^1\Pi_u$ are called **Lyman and Werner bands**.

Werner band: $C^1\Pi_u - X^1\Sigma_g^+$ at about 1100 Å;
Lyman band: $B^1\Sigma_u^+ - X^1\Sigma_g^+$ at about 1010 Å.

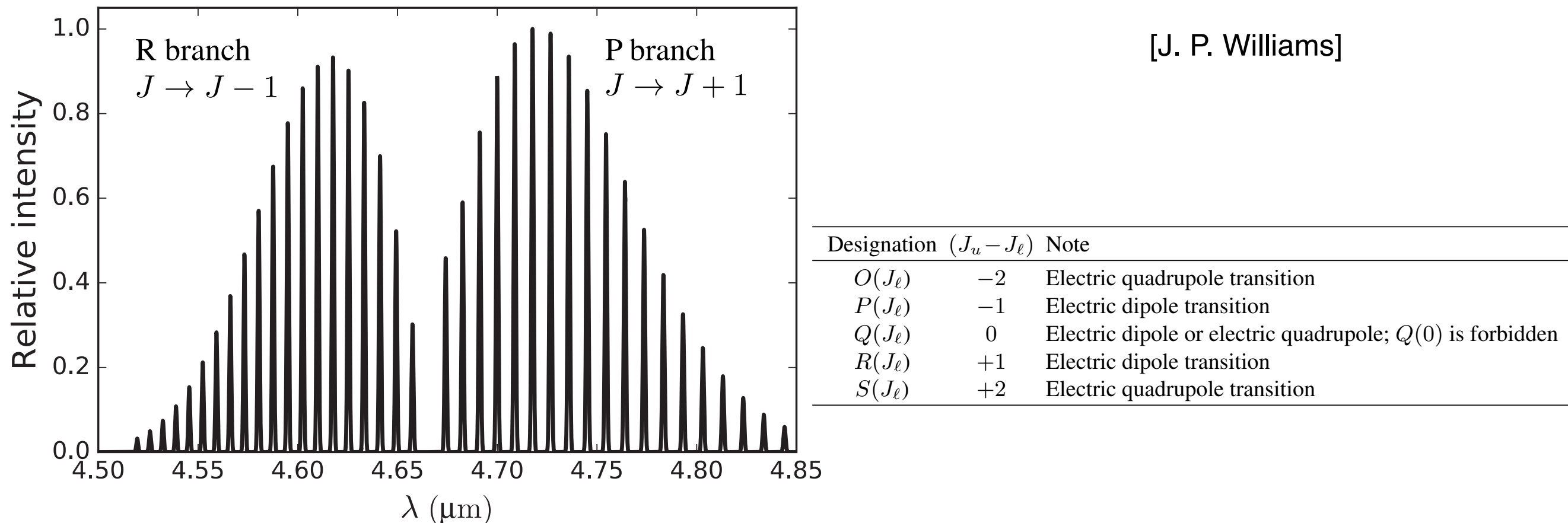
In principle, states are labelled alphabetically in ascending energy order. However, there are many exceptions. The lowest triplet state of H_2 is the $b^3\Sigma_u^+$ with the $a^3\Sigma_g^+$ lying somewhat higher.

[Energy levels of CO]



- The rotational and vibrational energy levels for carbon monoxide.
 - The left side shows the vibrational energy for each level v .
 - The rotational transitions are illustrated by the gray shading at each level.
 - The rotational energies are about 100 times smaller than the vibrational.
 - The inset on the right hand side shows a zoomed-in region of J-ladder.

[Energy levels of CO]



- Model spectrum of ro-vibrational lines for CO $v = 1 - 0$, illustrating the two branches corresponding to a positive or negative change in J and a central gap at $\Delta J = 0$.
 - The symmetry comes from the sign of the $\Delta J = \pm 1$ jump and produces two branches in the spectrum.
 - The R branch corresponds to a higher energy jump, $J \rightarrow J - 1$, and lies at shorter wavelengths.
 - The P branch is a smaller jump, $J \rightarrow J + 1$, and is at longer wavelengths.
 - The envelope shape arises from the population level distribution that is small at low levels due to the degeneracy $g_J = 2J + 1$, and at high levels due to the Boltzmann exponential $e^{E/kT_{\text{ex}}}$.
 - The difference between the relative intensity of the P and R branches is due to different values in the Einstein A coefficient.

The invisibility of H₂ in the Cold ISM

- Hydrogen is, by far, the most common element in the Universe and molecular hydrogen is the most common molecule in the ISM.
 - However, **its symmetry prevent pure rotational transitions**. From a quantum standpoint, the two hydrogen atoms are identical so there is no change in state in a 180 degree rotation. Because there is not separation of charge from the center of the system, it is also said to have **zero dipole moment**.
 - In cold regions, it will not radiate and is effectively invisible.

$$\text{dipole moment} = \sum_i q_i \mathbf{r}_i$$

- Tracers of Cold Molecular Gas
 - To diagnose the properties of these regions requires observations of other constituents: **dust and molecules such as CO**.
 - The offset between the charge distribution and center of mass in asymmetric molecules such as CO produces a dipole moment and a series of rotational energy levels that can be populated through collisions in cold gas.
 - Although the abundances of these molecules are very low relative to H₂, **they provide the only means for the gas to radiate** and result in a rich line spectrum at millimeter wavelengths.

- A sample of molecular rotational transitions
 - The following table shows a small set of commonly observed, low-lying, rotation transitions, $J + 1 \rightarrow J$, in the ground vibrational level, $v = 0$.
 - The Einstein A coefficients are extremely small compared to (permitted) vibrational and electronic transitions.
 - Higher transitions are excited by slightly warmer and denser gas.

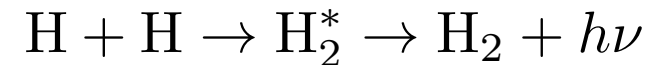
- The table includes the isotopologue, ^{13}CO of CO.
- Isotopologues are molecules that differ only in their isotopic composition. At least one atom has a different number of neutrons than the parent.
- They have the same transitions at nearby frequencies with similar decay and excitation rates.
- Observations of these rare species help diagnose conditions in dense regions where lines from the primary species are optically thick.

Molecule	Transition	ν (GHz)	E_u/k (K)	A (s^{-1})
CO	1–0	115.271	5.5	7.20×10^{-8}
	2–1	230.538	16.6	6.91×10^{-7}
	3–2	345.796	33.2	2.50×10^{-6}
	^{13}CO	1–0	110.201	5.3
		2–1	220.399	6.03×10^{-7}
		3–2	330.588	2.18×10^{-6}
CS	1–0	48.991	2.4	1.75×10^{-6}
	2–1	97.981	7.1	1.68×10^{-5}
	3–2	146.969	14.1	6.07×10^{-5}
HCN	1–0	88.633	4.3	2.41×10^{-5}
	2–1	177.261	12.8	2.31×10^{-4}
	3–2	265.886	25.5	8.36×10^{-4}
HCO^+	1–0	89.188	4.3	4.25×10^{-5}
	2–1	178.375	12.9	4.08×10^{-4}
	3–2	267.558	25.7	1.48×10^{-3}

Gas-Phase Formation of H₂

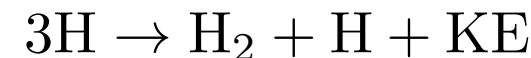
- ***Direct Radiative Association***

- When two free H atoms collide with each other, they create an excited hydrogen molecule that is unbound.



- It must emit a photon carrying away enough energy to leave it a bound state, or it will break apart again. There is no electric dipole moment. As a result, **there is no dipole radiation that could remove energy from the system and leave the two H atoms in a bound state**. Electric quadrupole transitions are possible, but the rates are very low.
 - As a consequence, the rate coefficient for direct radiative association of H₂ is so small that **this reaction can be ignored in astrochemistry**.

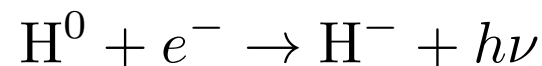
- ***Three-body reaction***



- The reaction can occur, when the third body carrying off the energy released when H₂ is formed, but the rate for this three-body reaction is negligible at interstellar or intergalactic densities.
 - At the high densities of a protostar or protoplanetary disk, the three-body reaction is able to convert H to H₂.

- ***Formation of negative hydrogen ion by radiative association followed by formation of H₂ by associative detachment:***

- First step:



- Second step:



This is an exothermic ion-molecule reaction.

- The density of negative H ion is very low because the formation rate of H⁻ (first step) is slow while there are many, rapid processes that destroy H⁻.

- ***In the absence of dust (e.g., in the early universe), H⁻ + H → H₂ + e⁻ is the dominant channel for forming H₂.***

Grain Catalysis of H₂

- The dominant process of H₂ formation in the Milky Way and other galaxies is via grain catalysis.

- The surface of a dust grain acts as a lab of chemical activity.

- **Adsorption:**

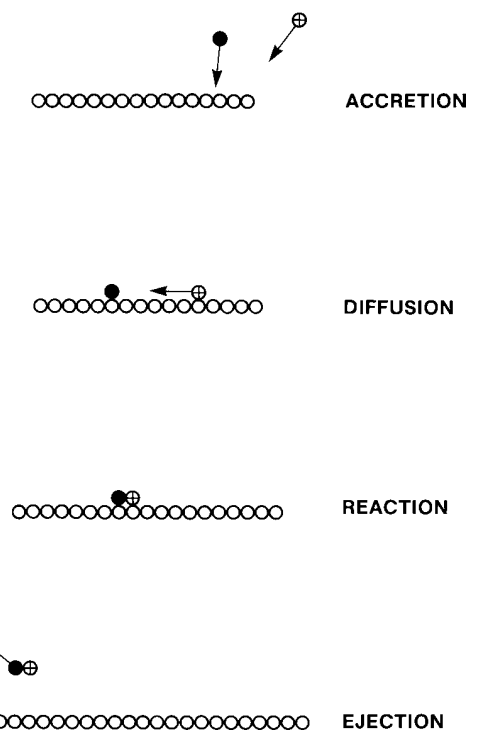
- ▶ A H atom colliding with a dust grain has some probability of sticking (bounding) to the grain.
- ▶ Sticking probability: $p_s \approx 0.3$ for grains with $a \sim 0.1\mu\text{m}$

- **Diffusion & Reaction:**

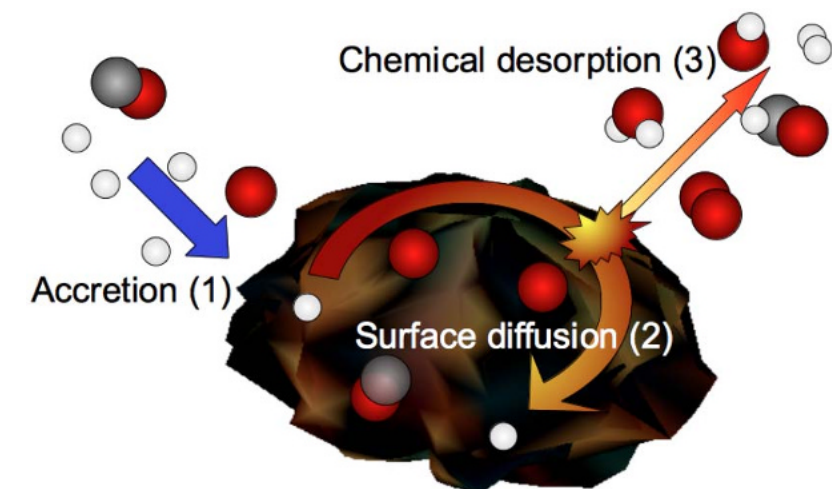
- ▶ Initially, the binding may be weak enough that the H atom is able to diffuse (i.e., random-walk) some distance on the grain surface, until it happens to arrive at a site where it is bound strongly enough that it becomes “trapped.”
- ▶ Subsequent H atoms arrive at random locations on the grain surface and undergoes their own random walks until they also become trapped, but eventually one of the newly arrived H atoms encounters a previously bound H atom before itself becoming trapped.
- ▶ When the two H atoms encounter one another, they react to form H₂.

- **Desorption:**

- ▶ The energy released when two free H atoms react to form H₂ in the ground state is $\Delta E = 4.5 \text{ eV}$. This energy is large enough to overcome the forces that were binding the two H atoms to the grain, and the H₂ molecule is ejected from the grain surface.



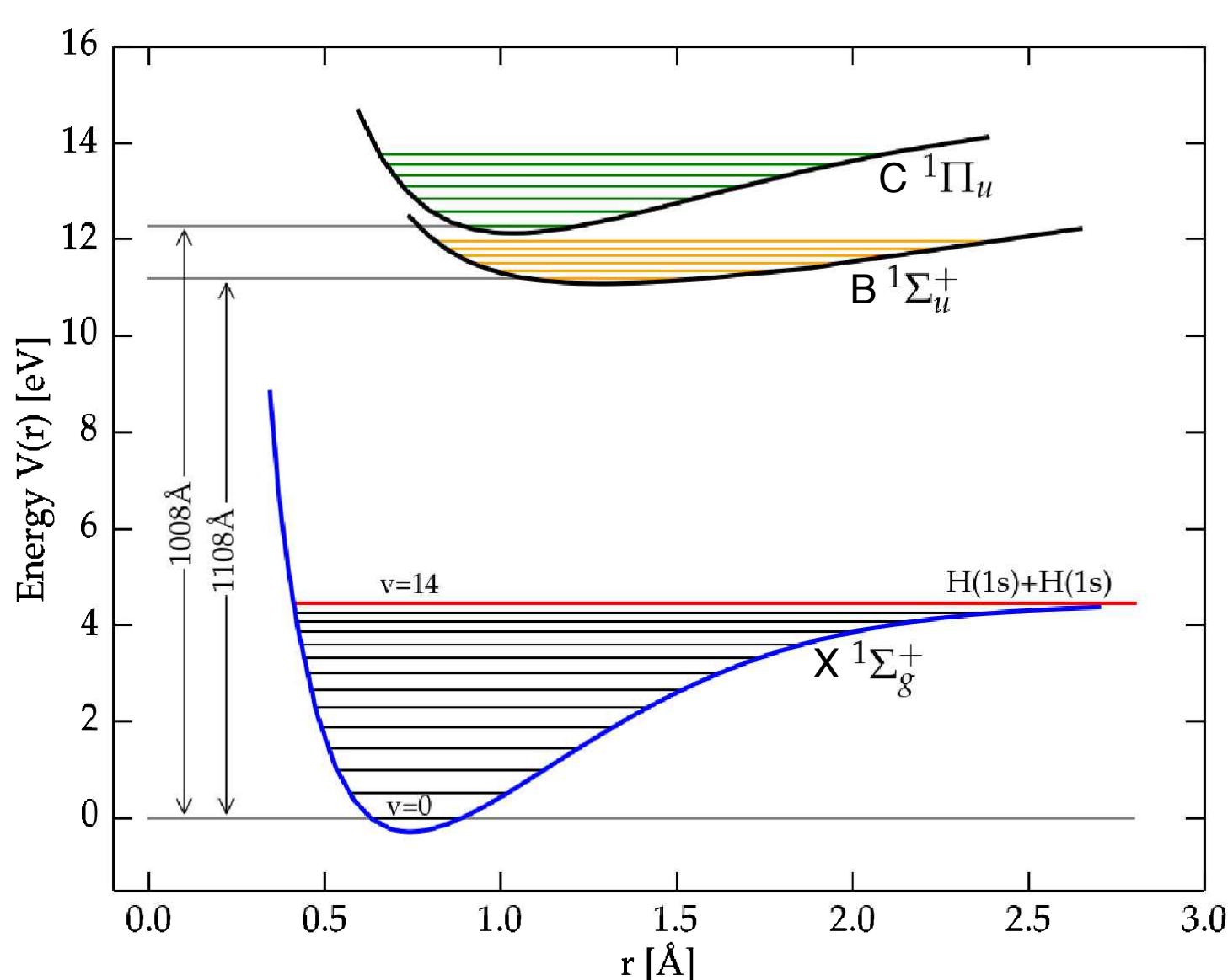
A schematic of the formation of molecules on grain surfaces. [Fig 4.1, Tielens]



Sketch that illustrates the chemical desorption process.
[Fig 1, Dulieu, 2003, Scientific Reports]

Photodissociation of H₂

- Photodissociation: $\text{H}_2 + h\nu \rightarrow \text{H} + \text{H} + \text{KE}$
 - Photodissociation is the principal process destroying interstellar H₂.

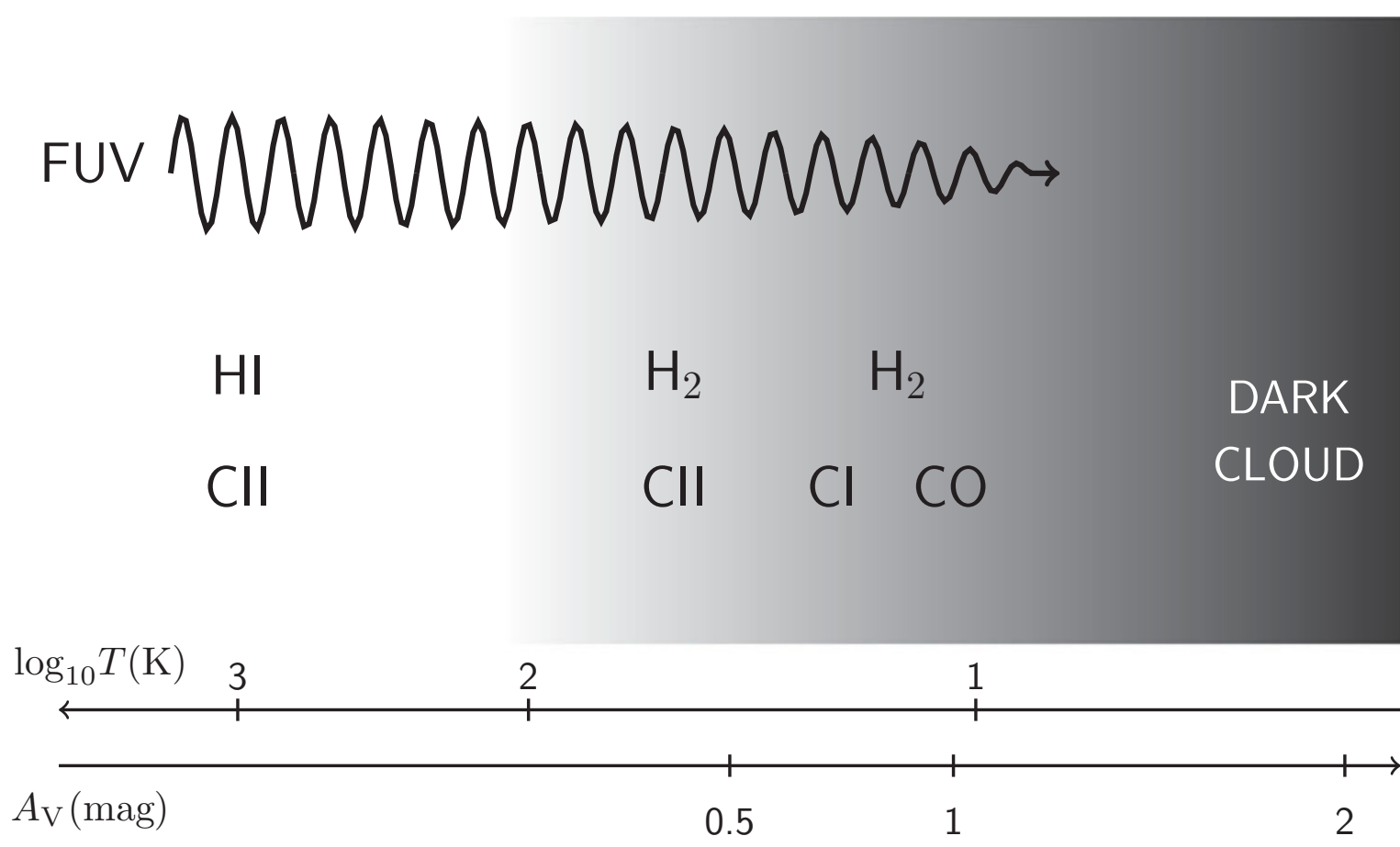


Schematic drawing of the potential energy curves of molecular hydrogen [Figure 7.4, Ryden]

- ▶ The first step is absorption of a resonance line photon ($\lambda = 912\text{-}1108\text{\AA}$), raising the H₂ from an initial level $X(v, J)$ to a level $B(v', J')$ or $C(v', J')$ of the first and second electronic states. This photoexcitation is via a permitted absorption line, and therefore the newly excited level is guaranteed to have electric dipole-allowed decay channels, with a large transition probability.
- ▶ The excited level is most likely to decay to vibrationally excited bound levels of the ground electronic state, and such decays occur $\sim 85\%$ of the time. However, a fraction of $\sim 15\%$ of the time, the downward spontaneous transition will be to the vibrational continuum ($v > 14$) of the ground electronic state: The two hydrogen atoms will then fly away from each other and the hydrogen molecule is dissociated.

PhotoDissociation Regions (PDRs)

- The edge of a molecular region, where molecules turn to atoms, is termed a **photodissociation region** or interchangeably a **photon dominated region**, both with the same PDR abbreviation.
 - Far-ultraviolet (FUV) radiation (91.2nm-200nm) can dissociate molecular hydrogen, ionize carbon, and broadly affect the physical properties and chemical composition of the gas.



The structure of a PDR. The FUV radiation enters from the left hand side into a neutral atomic cloud and is attenuated by dust to the point where molecular hydrogen begins to form in sufficient numbers to self-shield. Deeper in, carbon becomes neutral and then reacts with oxygen to form CO. Very little radiation penetrates further and more molecules form in the cold, dark interior.

[Fig. 7.11. J. P. Williams]

Molecular Clouds: Observations

- Cloud Structure
 - The ***clouds are very clumpy***, with the dense cores having typical sizes of < 1 pc or smaller, and densities $> 10^6 \text{ cm}^{-3}$.
 - The overall cloud extends for 3–20 pc on average, with a mean density of 10^{3-4} cm^{-3} .
 - Most molecular clouds show a number of discernible cores. These are often detected as sources of molecular lines with high critical densities (e.g., CS), while the general cloud is mapped using lines of lower critical density (mainly CO).
 - Within the galaxies, molecular clouds are most often seen organized into complexes with sizes from 20 pc to 100 pc, and overall H₂ masses of $10^{4-6} M_{\text{sun}}$. The distinction between “clouds” and “complexes” in terms of sizes and masses is somewhat artificial.
 - A more precise statement would be that ***we see a wide range of structures***, from single small clouds to large complexes of clouds, with many complexes arrayed along the spiral arms of the Galaxy.

Molecular Clouds: Cloud Categories

- Cloud Categories (based on the total surface density)
 - Individual clouds are separated into categories based on their optical appearance: **diffuse, translucent, or dark**, depending on the visual extinction A_V through the cloud.

Category	A_V (mag)	Examples
Diffuse Molecular Cloud	$\lesssim 1$	ζ Oph cloud, $A_V = 0.84^a$
Translucent Cloud	1 to 5	HD 24534 cloud, $A_V = 1.56^b$
Dark Cloud	5 to 20	B68 ^c , B335 ^d
Infrared Dark Cloud (IRDC)	20 to $\gtrsim 100$	IRDC G028.53-00.25 ^e

^a van Dishoeck & Black (1986).

^b Rachford et al. (2002).

^c Lai et al. (2003).

^d Doty et al. (2010).

^e Rathborne et al. (2010).

[Table 32.1, Draine]

- **Diffuse and translucent clouds** have sufficient UV radiation to keep gas-phase carbon mainly photo-ionized throughout the cloud.
 - ▶ Such clouds are usually pressure-confined, although self-gravity may be significant in some cases.
- The typical **dark clouds** have $A_V \sim 10$ mag, and is **self-gravitating**. Some dark clouds contain dense regions that are extremely opaque, with $A_V > 20$ mag.
- **Infrared Dark Clouds** are opaque even at 8 μm , and can be seen in silhouette against a background of diffuse 8 μm emission from PAHs in the ISM.

- Terminology for Cloud Complexes and Their Components

Categories	Size (pc)	n_{H} (cm^{-3})	Mass (M_{\odot})	Linewidth (km s^{-1})	A_V (mag)	Examples
GMC Complex	25 – 200	50 – 300	$10^5 – 10^{6.8}$	4 – 17	3 – 10	M17, W3, W51
Dark Cloud Complex	4 – 25	$10^2 – 10^3$	$10^3 – 10^{4.5}$	1.5 – 5	4 – 12	Taurus, Sco-Oph
GMC	2 – 20	$10^3 – 10^4$	$10^3 – 10^{5.3}$	2 – 9	9 – 25	Orion A, Orion B
Dark Cloud	0.3 – 6	$10^2 – 10^4$	5 – 500	0.4 – 2	3 – 15	B5, B227
Star-forming Clump	0.2 – 2	$10^4 – 10^5$	$10 – 10^3$	0.5 – 3	4 – 90	OMC-1, 2, 3, 4
Core	0.02 – 0.4	$10^4 – 10^6$	$0.3 – 10^2$	0.3 – 2	30 – 200	B335, L1535

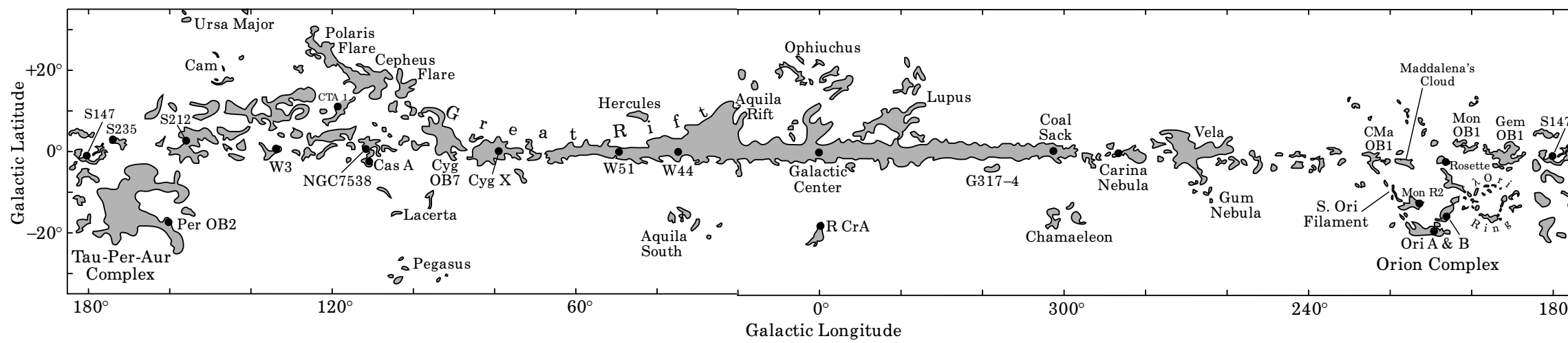
[Table 32.2, Draine]

- The **giant molecular cloud (GMC)** and **dark cloud** categories are distinguished mainly by total mass.
- Groups of distinct clouds are referred to as **cloud complexes**.
 - ▶ Molecular clouds are sometimes found in isolation, but ***in many cases molecular clouds are grouped together into complexes.***
 - ▶ Since large clouds generally have substructure, the distinction between “cloud” and “cloud complex” is somewhat arbitrary.
 - ▶ Delineation of structure in cloud complexes is guided by the intensities and radial velocities of molecular lines (e.g., CO J = 1-0) as well as maps of thermal emission from dust at submm wavelengths.

Categories	Size (pc)	n_{H} (cm^{-3})	Mass (M_{\odot})	Linewidth (km s^{-1})	A_V (mag)	Examples
GMC Complex	25 – 200	50 – 300	10^5 – $10^{6.8}$	4 – 17	3 – 10	M17, W3, W51
Dark Cloud Complex	4 – 25	10^2 – 10^3	10^3 – $10^{4.5}$	1.5 – 5	4 – 12	Taurus, Sco-Oph
GMC	2 – 20	10^3 – 10^4	10^3 – $10^{5.3}$	2 – 9	9 – 25	Orion A, Orion B
Dark Cloud	0.3 – 6	10^2 – 10^4	5 – 500	0.4 – 2	3 – 15	B5, B227
Star-forming Clump	0.2 – 2	10^4 – 10^5	$10 - 10^3$	0.5 – 3	4 – 90	OMC-1, 2, 3, 4
Core	0.02 – 0.4	10^4 – 10^6	$0.3 - 10^2$	0.3 – 2	30 – 200	B335, L1535

[Table 32.2, Draine]

- Structures within a cloud (self-gravitating entities) are described as **clumps**.
 - ▶ Clumps may or may not be forming stars; in the former case they are termed **star-forming clumps**. **Cores** are density peaks within star-forming clumps that will form a single star or a binary star.
$$R_{\text{clump}} > R_{\text{core}}$$
- GMC and GMC complex
 - ▶ Much of the molecular mass is found in large clouds known as “giant molecular clouds”, with masses ranging from $\sim 10^3 M_{\odot}$ to $\sim 2.5 \times 10^5 M_{\odot}$. These have reasonably well-defined boundaries.
 - ▶ A GMC complex is a gravitationally bound group of GMCs (and smaller clouds) with a total mass $\gtrsim 10^{5.3} M_{\odot}$.



Locations of prominent molecular clouds along the Milky Way

[Fig 32.2, Draine, Dame et al. (2001)]

Gas Surface Density in the Milky Way

- The most common way to study molecular gas is through molecular line emission, and the primary line used is the $J = 1-0$ transition (2.6 mm) of CO.
 - ▶ This transition is often optically thick, but the CO 1-0 luminosity of a cloud is approximately proportional to the total mass.
 - ▶ ***Velocity-resolved mapping of CO 1-0 together with an assumed rotation curve and an adopted value of the “CO to H₂ conversion factor” X_{CO} have been used to infer the surface density of H₂ over the Milky Way disk.***

Gas surface densities as a function of galactocentric radius. The Sun is assumed to be at $R = 8.5$ kpc.

- Surface density of H₂ estimated from CO 1-0 observations (Nakanishi & Sofue 2006), assuming
 $X_{CO} = 1.8 \times 10^{20} \text{ H}_2 \text{ cm}^{-2}/\text{K km s}^{-1}$
- Surface density of H II derived from pulsar dispersion measures (Cordes & Lazio 2003).
- Surface density of H I from 21-cm studies (Nakanishi & Sofue 2003)

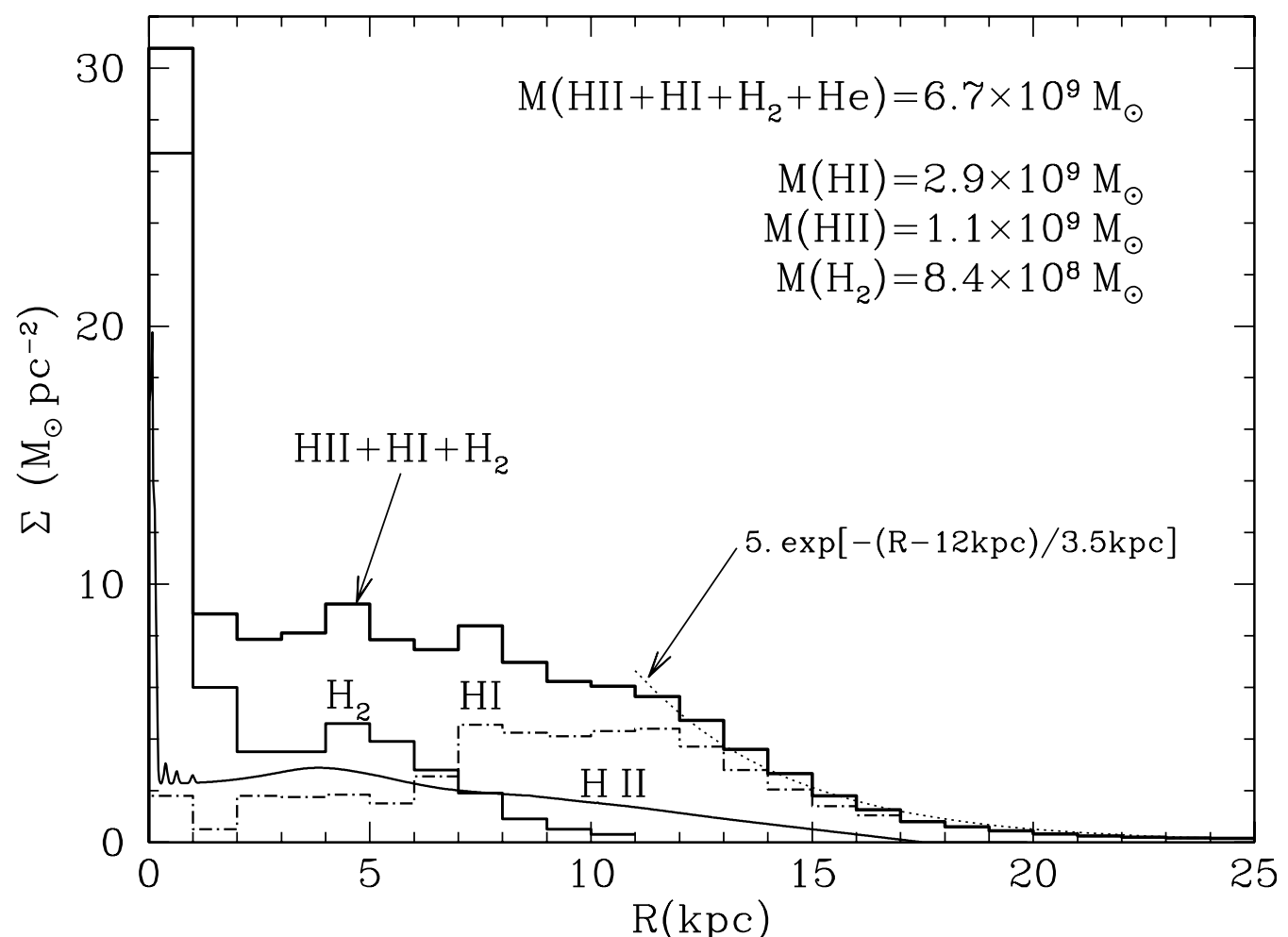


[Fig 32.4, Draine]

Dust

Dust matters!

- Importance of Dust
 - In our Galaxy, **the gas-to-dust ratio is about 100:1 by mass.** Since the ISM is about 10% of the baryonic mass of the Galaxy, dust grains comprise roughly 0.1% of the total baryonic mass.
 - Dust grains absorb roughly 30-50% of the starlight emitted by the Galaxy and re-emit it as far-infrared continuum emission. ***This means that only 0.1% of the baryons are ultimately responsible for a third to a half of the bolometric luminosity of the Galaxy.***
 - Dust grains are central to the chemistry of interstellar gas. ***The abundance of H₂ in the ISM can only be understood if catalysis on dust grains is the dominant formation avenue.***
 - The formation of planetary systems is believed to begin when dust grains in a protostellar disk begin to coagulate into larger grains, leading to planetesimals and eventually to planets, carrying their complex organic molecules with them.

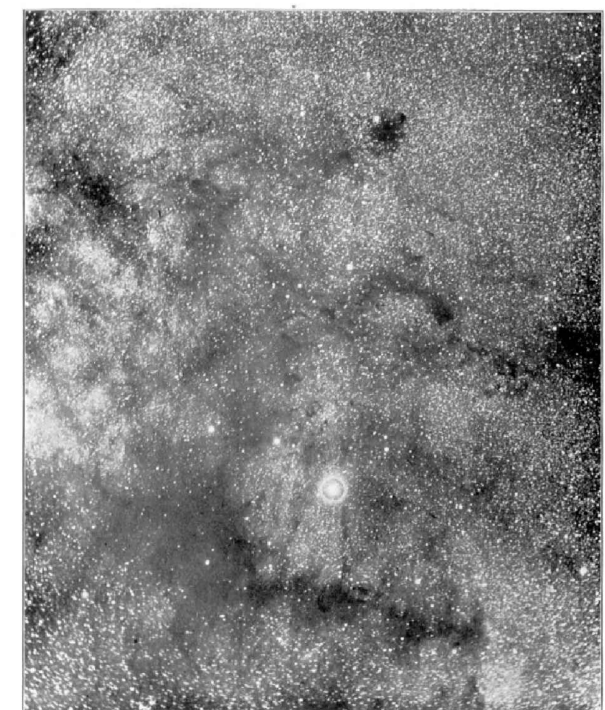
Observed Properties

- **Extinction = Absorption + Scattering**
 - Dust particles can scatter light, changing its direction of propagation. When we look at a reflection nebula, like that surrounding the Pleiades, we are seeing light from the central stars that has been scattered by dust into our line of sight.
 - Dust particles can also absorb light. The relative amount of scattering and absorbing depends on the properties of the dust grains.
- **Thermal radiation from Dust**
 - When dust absorbs light, it becomes warmer, so dust grains can emit light in the form of thermal radiation. Most of this emission is at wavelengths from a few microns (near IR) to the sub-mm range (Far-IR).
- **Polarization**
 - The polarization of starlight was discovered in 1949 (Hall 1949).
 - The degree of polarization tends to be larger for stars with greater reddening, and stars in a given region of the sky tends to have similar polarization directions.



The Pleiades cluster and surrounding reflection nebulae (Fig. 6.3, Ryden)

PLATE II.



PHOTOGRAPH OF THE MILKY WAY NEAR THE STAR THETA OPHIUCHI.

The dark structures near θ Ophiuchi
(Barnard 1899; Fig. 6.1, Ryden)

Extinction

- ***Extinction***

- Astronomers characterize the attenuating effects of dust by the “extinction” A_λ at wavelength λ . The extinction at a particular wavelength λ , measured in “magnitudes” is defined by the difference between the observed magnitude m_λ and the unabsorbed magnitude m_λ^0 :

$$\begin{aligned} A_\lambda \text{ [mag]} &= m_\lambda - m_\lambda^0 \\ &= -2.5 \log_{10} \left(\frac{F_\lambda}{F_\lambda^0} \right) \end{aligned}$$

F_λ = the observed flux from the star

F_λ^0 = the flux that would have been observed if the only attenuation had been from the inverse square law.

- The extinction measured in magnitudes is proportional to the optical depth:

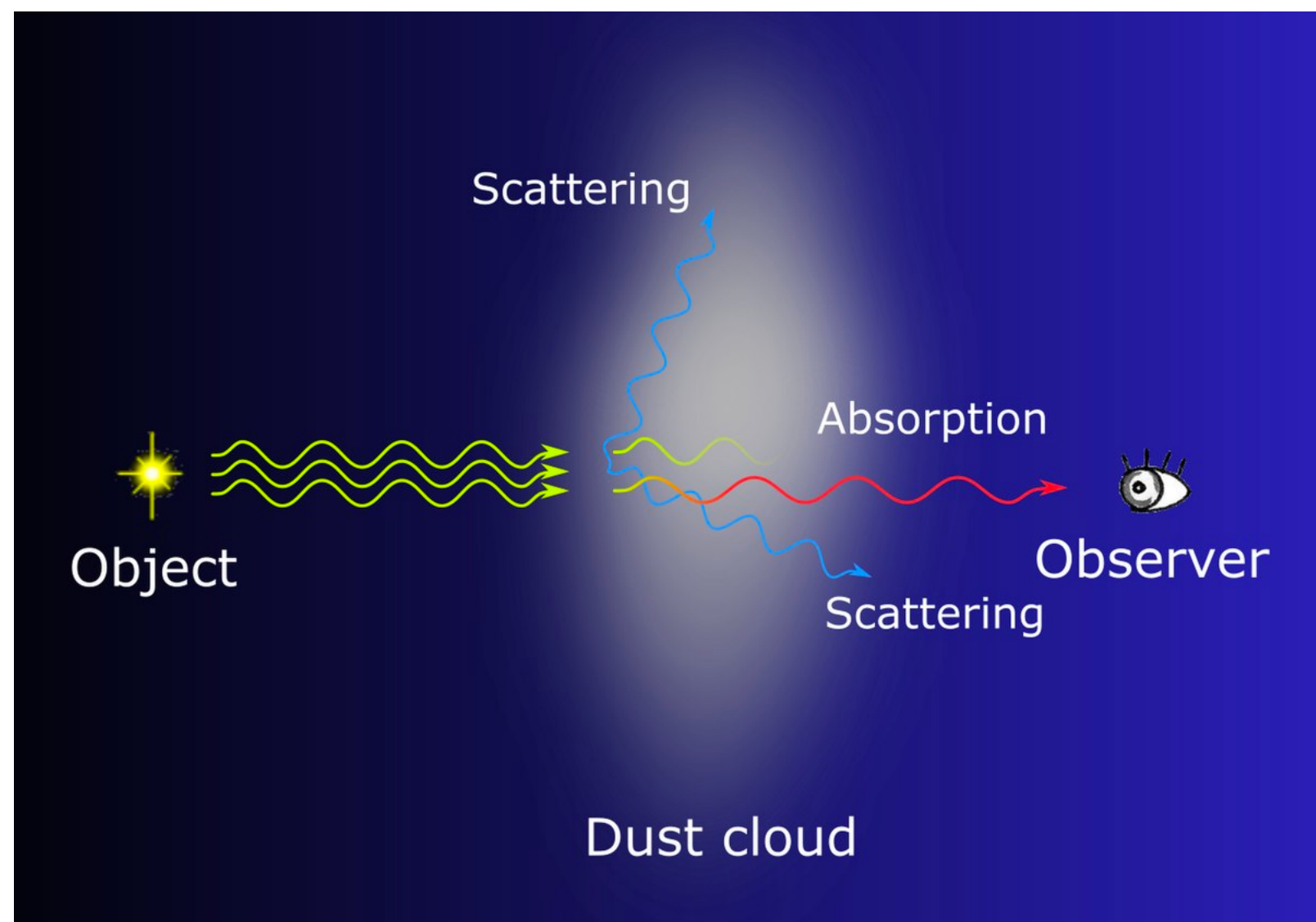
$$F_\lambda = F_\lambda^0 e^{-\tau_\lambda}$$



$$\begin{aligned} A_\lambda &= 2.5 \log_{10} (e^{\tau_\lambda}) = 2.5 \log (e) \times \tau_\lambda \\ &= 1.086 \tau_\lambda \end{aligned}$$

Reddening

- **Reddening**
 - Reddening is the phenomena of the color of a visible astronomical object (e.g., star) appearing more red from a distance than from nearby.
 - Within the visible wavelength range, **the absorption/scattering cross-section by dust increases with frequency, absorbing/scattering more of the blue light than red.**
 - This effect leads to the reddening.



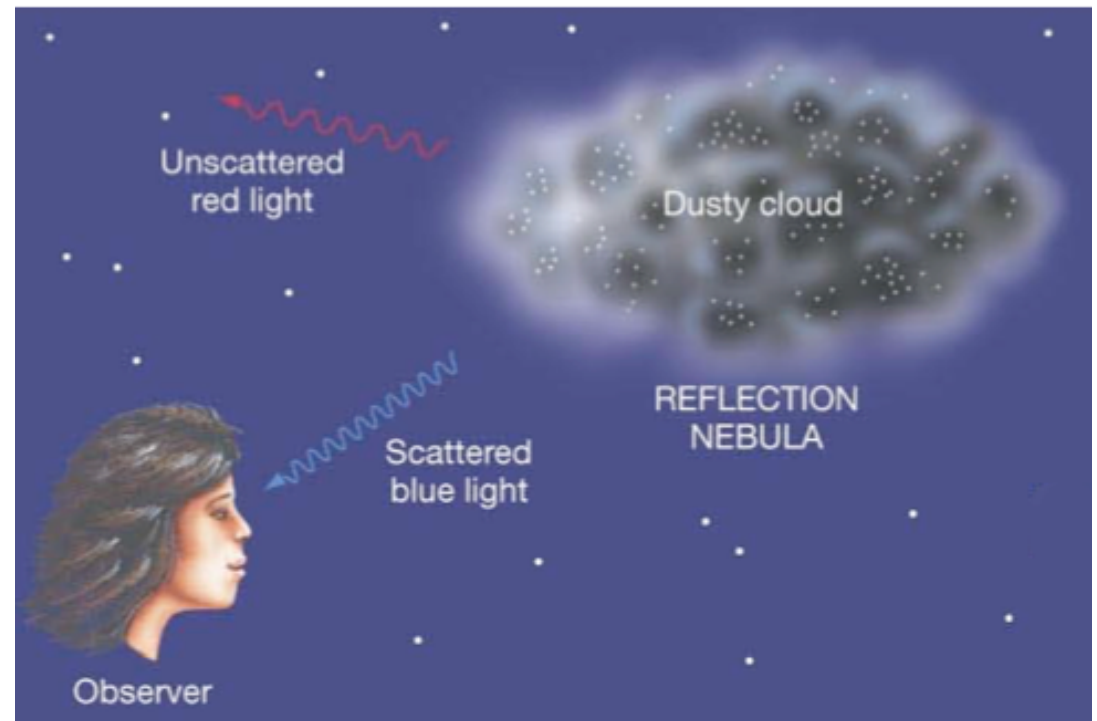
Blue Reflection Nebulae

- ***Scattering of Starlight***

- When an interstellar cloud happens to be unusually near one or more bright stars, we have a reflection nebula, where we see starlight photons that have been scattered by the dust in the cloud.

- ***The spectrum of the light coming from the cloud surface shows the stellar absorption lines***, thus demonstrating that scattering rather than some emission process is responsible.

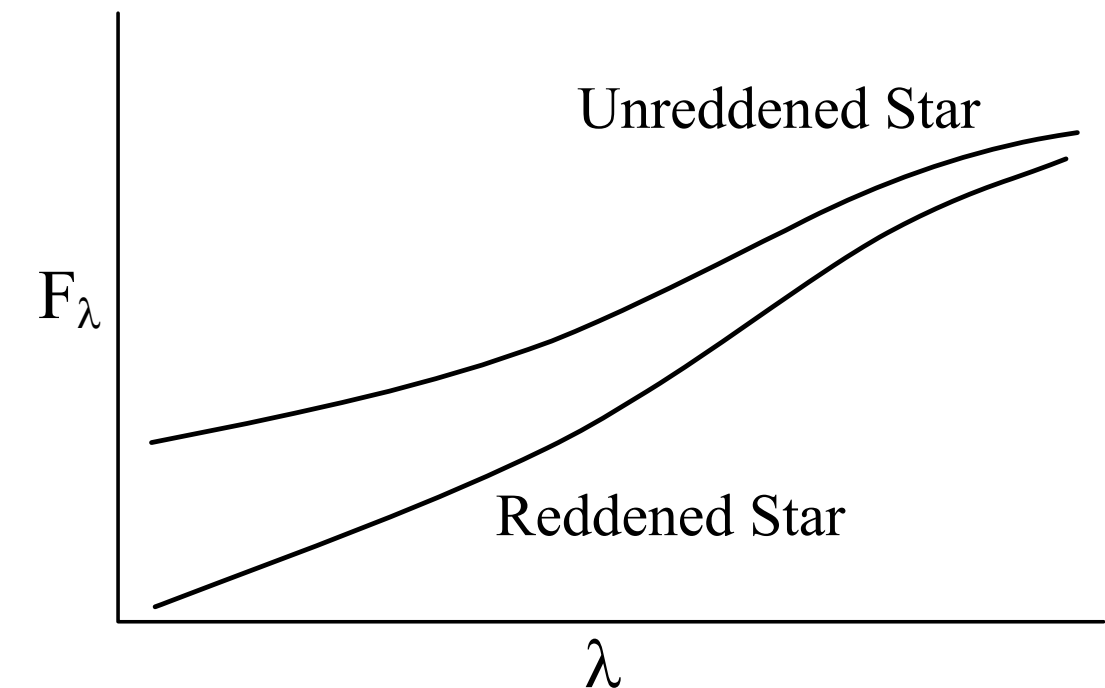
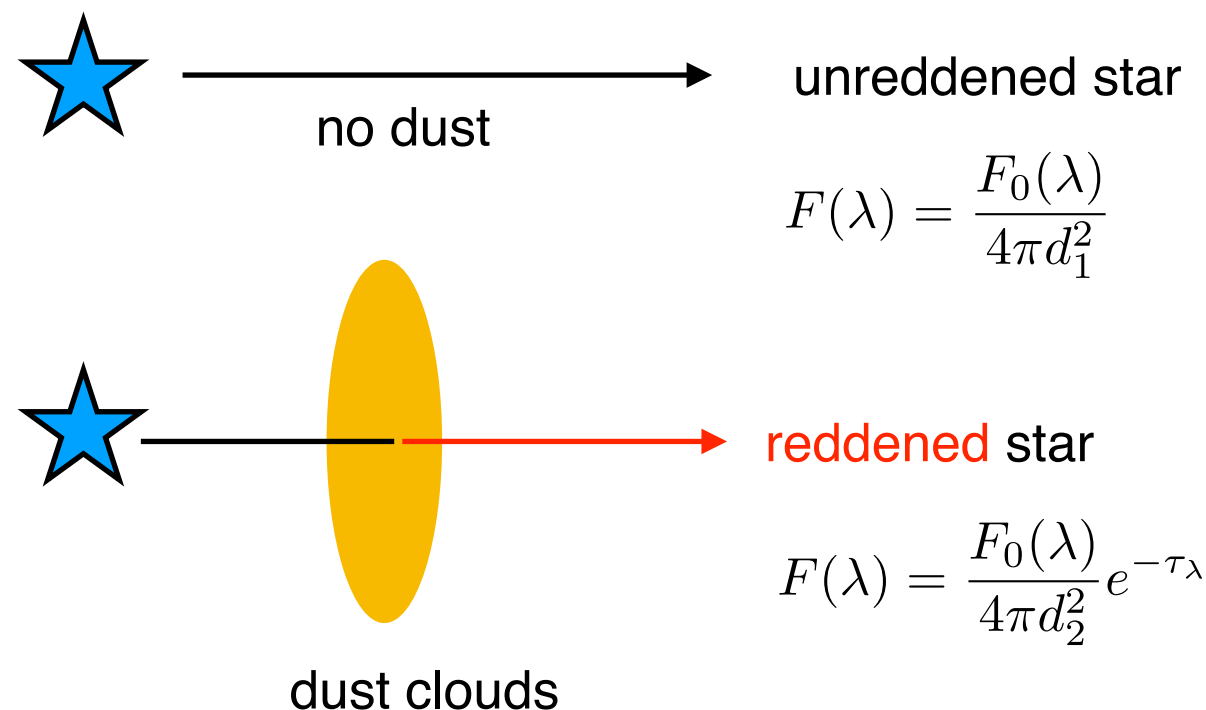
- Given the typical size of interstellar dust grains, blue light is scattered more than red light. ***A reflection nebulae is typically blue*** (so for the same reason that the sky is blue, except it's scattering by dust (for the reflection nebula) vs by molecules (for the earth's atmosphere)).



How to measure the Interstellar Extinction

- Pair method
 - Trumpler (1930) compared the spectra of pairs of stars with identical (or similar) spectral type, one with negligible obscuration and the other extinguished by dust along the line of sight. This method remains our most direct way to study the “selective extinction” or “reddening” of starlight by the interstellar dust.

Compare two stars
with the same spectral type



• ***The Reddening Law, Extinction Curve***

- Extinction curve - the extinction A_λ as a function of wavelength or frequency
 - ▶ A typical extinction curve shows the ***rapid rise in extinction in the UV***.
 - ▶ ***The extinction increases from red to blue***, and thus the light reaching us from stars will be “reddened” owing to greater attenuation of the blue light.
 - ▶ The reddening by dust is expressed in terms of a ***color excess***; for instance,

B-V color excess:

$$E(B - V) \equiv A_B - A_V$$

$\lambda_B \sim 4400 \text{ \AA}$
 $\lambda_V \sim 5500 \text{ \AA}$

in general,

$$E(\lambda_1 - \lambda_2) \equiv A_{\lambda_1} - A_{\lambda_2} \quad (\lambda_1 < \lambda_2)$$

- ▶ The detailed wavelength dependence of the extinction - the “***reddening law***” - is sensitive to the ***composition*** and ***size distribution*** of the dust particles.
- ▶ The slope of the extinction at visible wavelengths is characterized by the dimensionless ratio, ***the ratio of total to selective extinction***:

$$R_V \equiv \frac{A_V}{A_B - A_V} \equiv \frac{A_V}{E(B - V)}$$

- ▶ R_V ranges between 2 and 6 for different lines of sight. Sightlines through diffuse gas in the Milky Way have $R_V \approx 3.1$ as an average value. ***Sightlines through dense regions tend to have larger values of R_V*** . In dense clouds, the value $R_V \approx 5$ is typically adopted.

- ▶ ***Observed extinction curves vary in shape from one line of sight to another.***
- ▶ Extinction curve, relative to the extinction in the I band ($\lambda = 8020\text{\AA}$), as a function of inverse wavelength, for Milky Way regions characterized by different values of R_V .

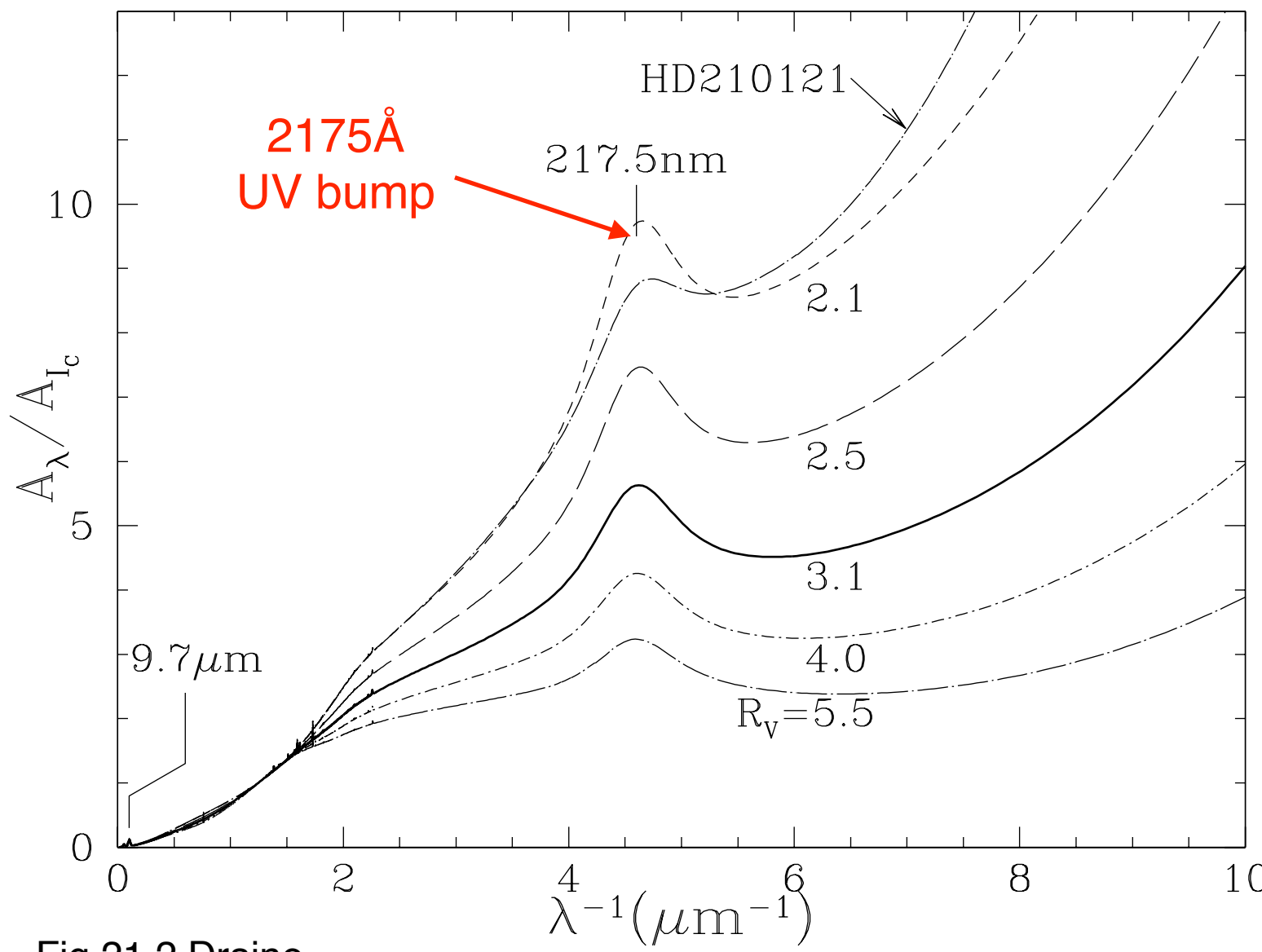


Fig 21.2 Draine

Parameterization of the extinction curve.

Cardelli et al. (1989)

Fitzpatrick (1999)

Gas-to-dust ratio

- If the dust grains were large compared to the wavelength, we would be in the “geometric optics” limit, and the extinction cross section would be independent of wavelength (gray extinction).
 - ▶ The tendency of the extinction to rise with decreasing λ , even at the shortest ultraviolet wavelengths tells us that grains smaller than the wavelength must be making an appreciable contribution to the extinction at all observed wavelengths, down to $\lambda = 0.1 \mu\text{m}$.
 - ▶ According to the Mie theory, “small” means (approximately) that $2\pi a/\lambda \lesssim 1$. Thus interstellar dust must include a large population of small grains with $a \lesssim 0.015 \mu\text{m}$.
- The dust appears to be relatively well-mixed with the gas (Bohlin et al. 1978; Rachford et al. 2009):

$$\frac{N_{\text{H}}}{E(B-V)} = 5.8 \times 10^{21} \text{ H cm}^{-2} \text{ mag}^{-1}$$

Gas-to-dust ratio $\approx 100 - 200$ by mass

- ▶ For sightlines with $R_V \approx 3.1$, this implies that

$$\frac{A_V}{N_{\text{H}}} \approx 5.3 \times 10^{-22} \text{ mag cm}^2 \text{ H}^{-1}$$

column density of total hydrogen nuclei
 $N_{\text{H}} \equiv N(\text{HI}) + 2N(\text{H}_2)$

- ▶ Thus, even at high galactic latitudes, where the column density of hydrogen is $\sim 10^{20} \text{ cm}^{-2}$, there is still some foreground extinction when looking at extragalactic sources; ~ 0.05 magnitudes in the V band.

- ***Mean ratio of visual extinction to length in the Galactic plane***

$$\left\langle \frac{A_V}{L} \right\rangle \approx 1.8 \text{ mag kpc}^{-1}$$

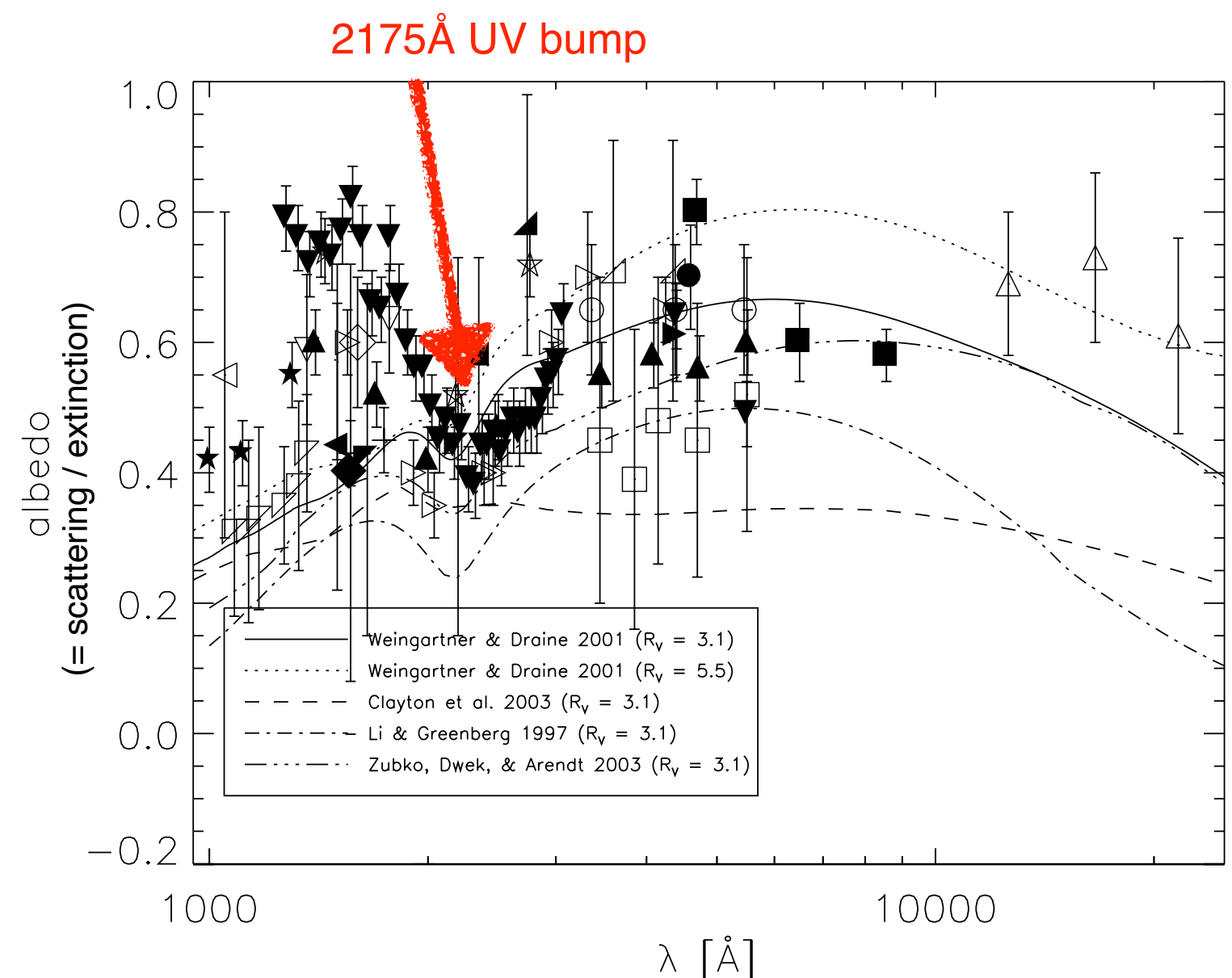
UV bump

- The study of dust scattering properties has shed light on the nature of the 2175Å bump and the far-ultraviolet rise features of extinction curves.
- Lillie & Witt (1976) and Calzetti et al. (1995) showed that ***the 2175Å bump was likely an absorption feature with “no scattering component.”***

The determinations of the albedo in reflection nebulae, dark clouds, and the diffuse Galactic light are plotted versus wavelength.

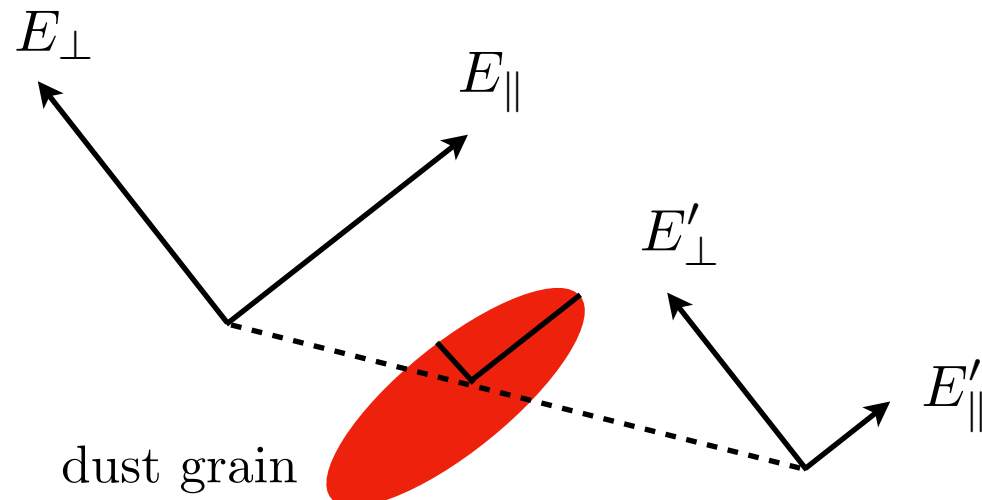
Predictions from dust grain models are also plotted for comparison.

Karl D. Gordon (2004, ASPC, 309, 77)



- **Polarization of Starlight by Interstellar Dust**

- Initially unpolarized light propagating through the ISM becomes linearly polarized as a result of ***preferential extinction*** of one linear polarization mode relative to the other.

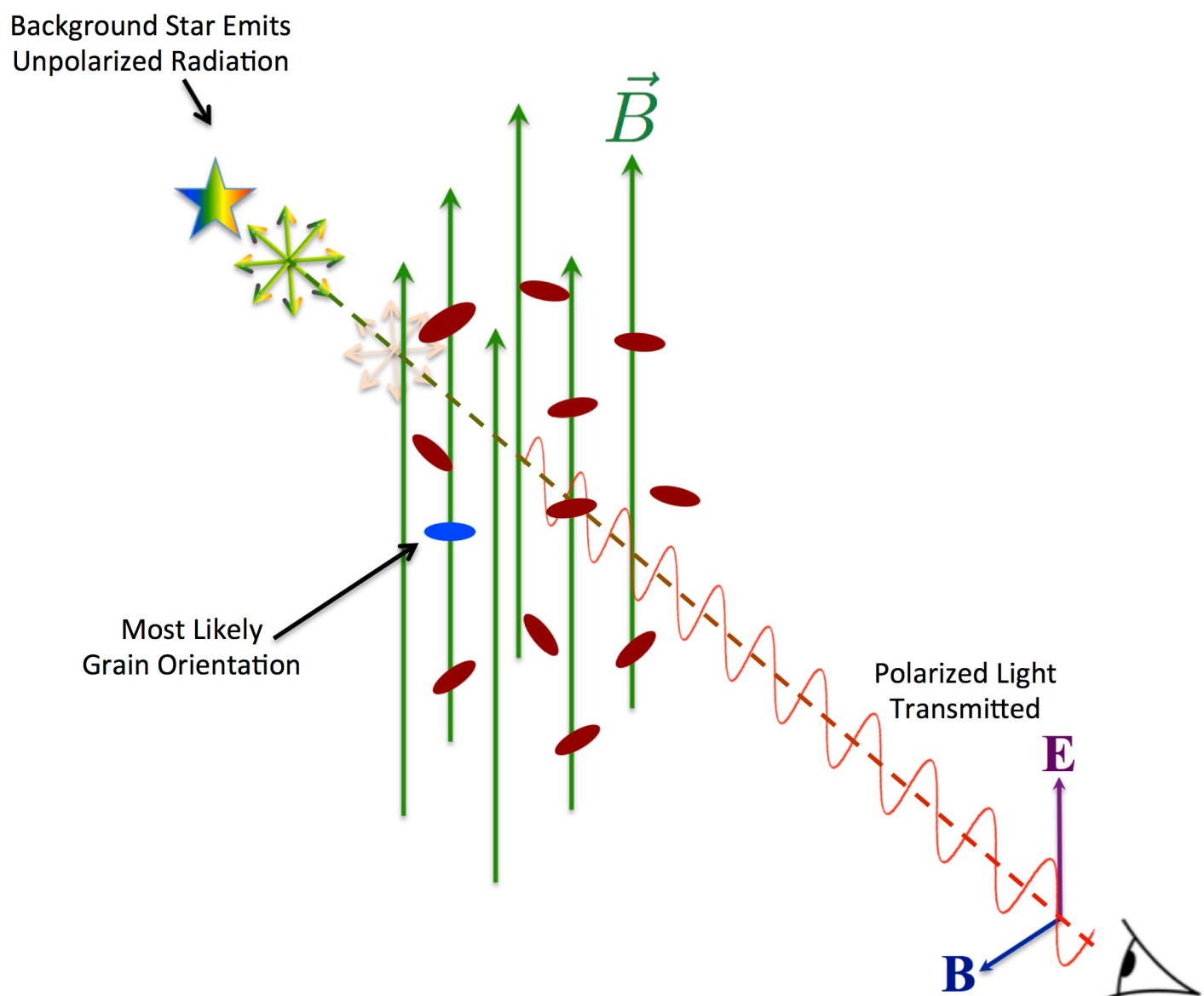


$$\begin{aligned} E_{\parallel} &= E_{\perp} \\ E'_{\parallel} &< E'_{\perp} \end{aligned}$$

$$\begin{aligned} E'_{\parallel} &= E_{\parallel} e^{-\tau_{\parallel}} \\ E'_{\perp} &= E_{\perp} e^{-\tau_{\perp}} \\ \tau_{\parallel} &> \tau_{\perp} \end{aligned}$$

The starlight is slightly more blocked along the long axis of the grains than along the short axis.

This give rise to the polarization of starlight along the short axis.



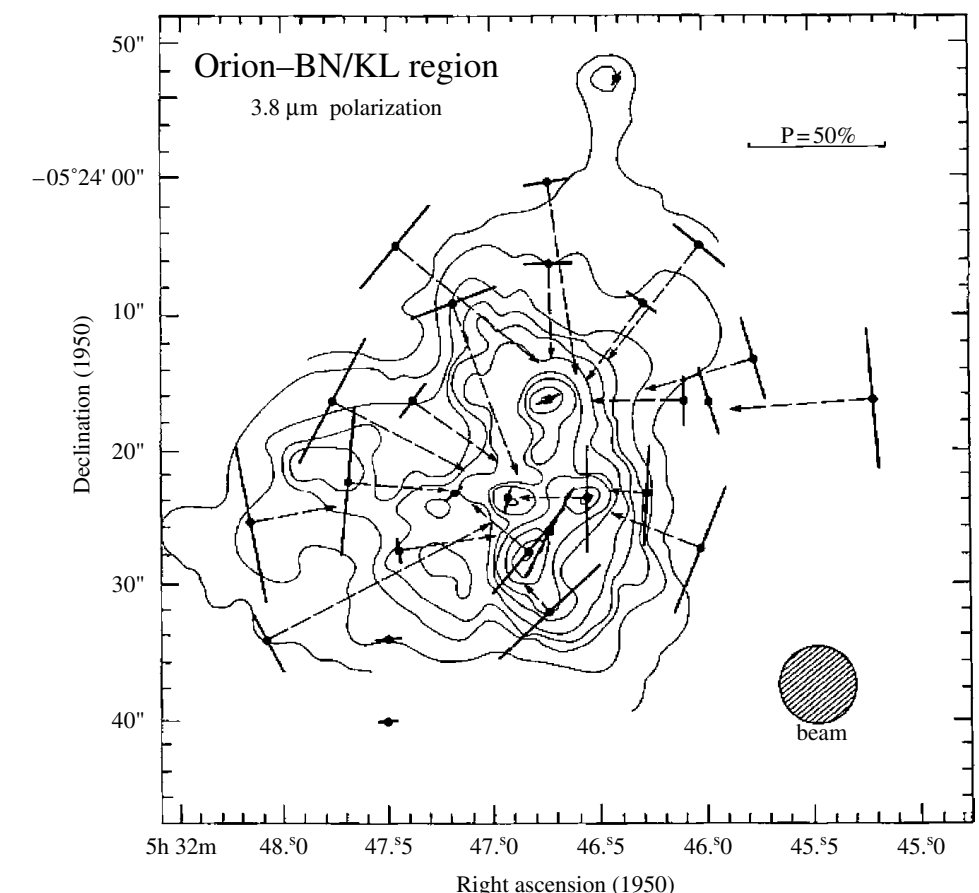
credit: B-G Andersson

- **Polarized Infrared Emission**

- The far-IR emission from aligned dust grains will also be polarized, this time **with a direction along the long axis of the grains**. Far-IR polarization has been observed for a large number of molecular clouds that have “high” dust emission optical depths at long wavelengths ($\sim 0.1\text{-}1$ mm).

- **Polarization due to scattering**

- Scattering of light by dust grains generally also lead to polarization.
- For single scattering, **the polarization vector is perpendicular to the line connecting the light source and the scattering grain**.
- The degree of polarization and its distribution provide information on the characteristics of the scattering grains and the geometry of the nebula.



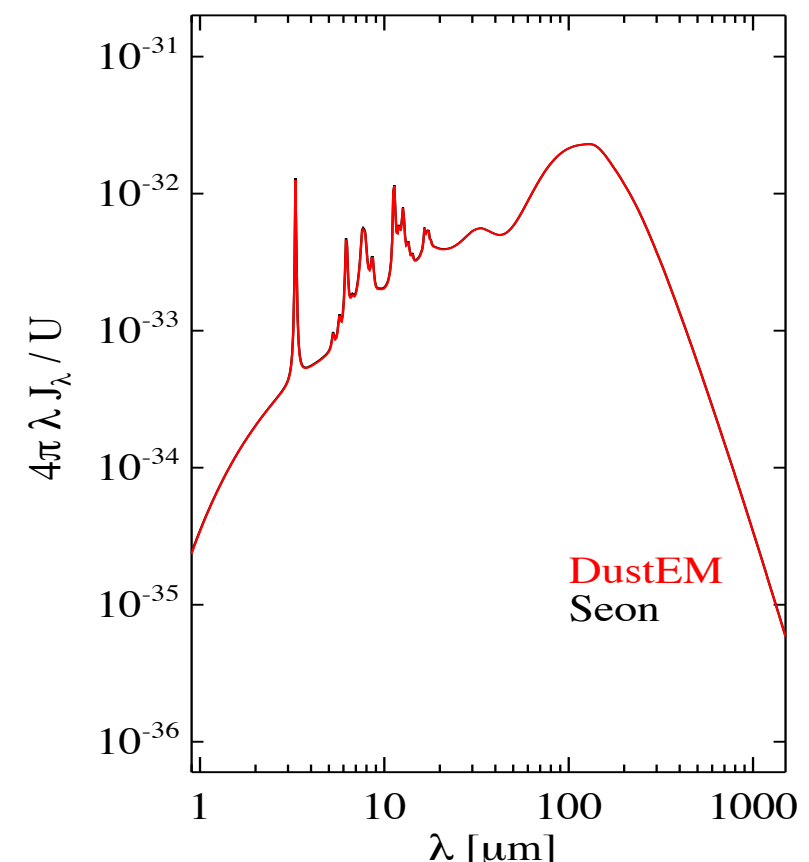
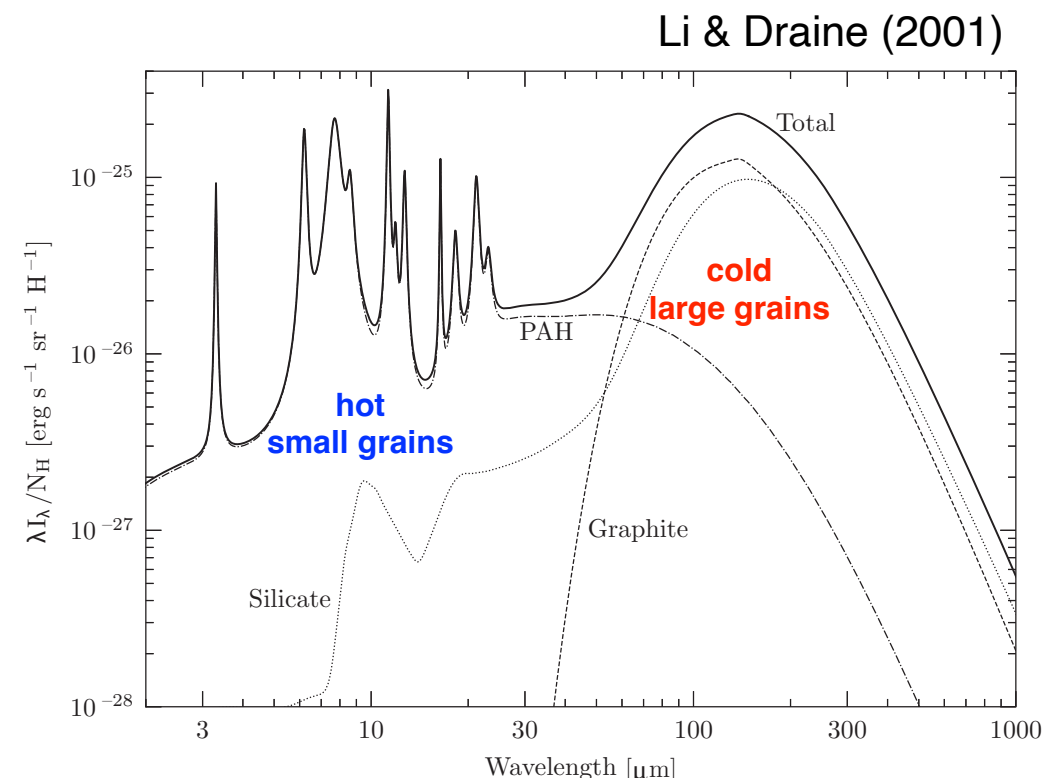
Linear polarization of the IR reflection nebula associated with the region of massive star formation in Orion.
The linear polarization vectors measured at K are superimposed on a map of the scattered light intensity.

[Werner et al. 1983, ApJ, 265, L13]

Infrared Emission

- ***Infrared Emission***

- Dust grains are heated by starlight, and cool by radiating in the infrared.
- The IR spectrum provides very strong constraints on grain models.
- There are two components: ***a cold ($T \sim 15\text{-}20\text{ K}$) component*** emitting mainly at long wavelengths (far-IR) and ***a hot ($T \sim 500\text{ K}$) component*** dominating the near- and mid-IR emission.
 - ▶ The **cold component** is due to **large dust grains** in radiative equilibrium with the interstellar radiation field.
 - ▶ The **hot component** is due to **ultra small grains** and **PAH species** that are heated by a single UV photon to temperatures of $\sim 1000\text{ K}$ and cool rapidly in the near- and mid-IR.



Homework (due date: 03/31)

- [Q3]

- Suppose that we observe a radio-bright QSO and detect absorption lines from Milky Way gas in its spectra. The 21 cm line is seen in optically-thin absorption with a profile with $\text{FWHM}(\text{H I}) = 10 \text{ km s}^{-1}$. We also have high-resolution observations of the Na I doublet lines referred to as D_1 (5898\AA) and D_2 (5892\AA) in absorption. The Na I D_2 5892\AA line width is $\text{FWHM}(\text{Na I } D_2) = 5 \text{ km s}^{-1}$. The line profiles are the result of a combination of thermal broadening plus turbulence with a Gaussian velocity distribution with one-dimensional velocity dispersion $\sigma_{v, \text{turb}}$.

You will want to employ the following theorem: If the turbulence has a Gaussian velocity distribution, the overall velocity distribution function of atoms of mass M will be Gaussian, with one-dimensional velocity dispersion:

$$v_{\text{rms}}^2 = \sigma_{\text{turb}}^2 + \frac{2kT}{M}$$

- Suppose that the Na I D_2 line is optically thin, and calculate the kinetic temperature T and $\sigma_{v, \text{turb}}$.
- [Note]
 - ▶ $\text{FWHM} = 2\sqrt{2 \ln 2}\sigma$ for a Gaussian function.
 - ▶ The atomic number of Na is 11. Use the mass of its stable isotope.

[Q4]

Look up (google) the absolute magnitude of the Sun at V band. What would the apparent magnitude be for a solar twin at the Galactic center? What would it be with dust assuming that the extinction along the Galactic plane is 1 mag/kpc?